Author's Response

28 October 2018

Reviewer: 1

Comments:

This paper examines aerosol mass scattering efficiencies using a chemical transport model and ground-based aerosol composition data. The work is important because aerosol mass scattering efficiencies are required to estimate aerosol radiative properties- both for surface and satellite-derived properties. Understanding model biases as a function of aerosol size and hygroscopic effects is necessary for accurate estimates of aerosol optical properties. The authors 'tune' the model to observations to determine the aerosol size and hygroscopic properties that most closely agree with observations. While the paper is fairly clearly written, it could benefit from clarifications in the method description, as described in the comments below. One of the major weaknesses of the paper is the lack of comparisons of observed and modeled mass concentrations and light scattering coefficients. Since mass scattering efficiencies are calculated by dividing light scattering by mass, it is important to understand if the model is accurately estimating either of those before attempting to minimize error in size or hygroscopicity. If the model cannot get those parameters correctly, adjusting size or hygroscopicity may be accounting for other errors. Does the model accurately estimate dry conditions? Are the errors in the observations accounted for? I recommend publication after addressing detailed comments below.

Thank you for the positive comments. There seems to be a misunderstanding regarding our methods. The purpose of the manuscript is to evaluate mass scattering efficiency since that is largely assumed in GEOS-Chem. Modeled mass scattering efficiency is not calculated from modeled mass and b_{sp}, so evaluation of modeled mass and b_{sp} is a separate question. Rather than using modeled light scattering and mass to calculate mass scattering efficiencies, we calculate mass scattering efficiency using IMPROVE speciation measurements alongside aerosol physical and optical properties from the model. This removes the influence of possible biases in model mass or composition from the analysis. Thus the comparison of modeled and measured mass concentrations and b_{sp} are irrelevant. The purpose of the manuscript is to evaluate mass scattering efficiency since that is largely assumed in GEOS-Chem. Modeled mass scattering efficiency is not calculated from modeled mass and b_{sp}, so evaluation of modeled mass and b_{sp} is a separate question. We clarified this in the manuscript:

Page 4 Line 8-12: "The majority of our analysis focuses on the accuracy of the GEOS-Chem parameterization of mass scattering efficiency based on optical parameters given in Table A1. These default aerosol physical and optical properties are defined by the Global Aerosol Data Set (GADS) (Koepke et al., 1997), as implemented by Martin et al. (2003), with modifications to dry size distributions (Drury et al., 2010) and dust mass partitioning (Ridley et al., 2012). After evaluating and improving this parameterization, implications are examined using the full GEOS-Chem simulation in section 3.3."

Further clarifications in the methods are provided below.

Specific Comments:

Pg 1:16, Does this reduction correspond to all of North America?

Errors in observations are accounted for as discussed in detail below.

The overall bias is reduced from 82% to 9% in dry conditions. This takes into account all sites in North America. The words “overall” and “at IMPROVE sites” have been added into this sentence to clarify:

Page 1 Line 14-17: “Inhibiting hygroscopic growth of SIA below 35% RH and decreasing the dry geometric mean radius, from 0.069 µm for SIA and 0.073 µm for OA to 0.058 µm for both aerosol types, significantly decreased the overall bias observed at IMPROVE sites in dry conditions from 82% to 9%.”

Pg 1:17-20, Are these reductions also reflecting the size shift or just the use of kappa?

Clarification has been added to indicate that these changes reflect both the size shift and the use of kappa.

Page 1 Line 19-22: “Incorporating these changes in aerosol size and hygroscopicity into the GEOS-Chem model resulted in an increase of 16% in simulated average α_{sp} over North America, with larger increases of 25% to 45% in northern regions with high RH and hygroscopic aerosol fractions, and decreases in α_{sp} up to 15% in the southwestern U.S. where RH is low.”

Pg 2:4, Perhaps “expansion” is a more accurate term than “growth”?

“growth” has been changed to “expansion” (now Page 2 Line 9)

Pg 2:7, Remove “fine” before “particulate mass concentrations” because this is followed by 10 um and add “PM2.5” before “chemical composition” to be clear that PM10 is not speciated.

Thank you, these changes have been made.

Page 2 Line 10-13 “The Interagency Monitoring of Protected Visual Environments (IMPROVE) network offers long-term collocated measurements since 1987 of particle scatter (b_{sp}), relative humidity (RH), particulate mass concentrations less than 10 µm (PM_{10}) and less than 2.5 µm ($PM_{2.5}$) as well as $PM_{2.5}$ chemical composition at sites across the United States and Canada (Malm et al., 1994; Malm et al., 2004).

Pg 2:9, Replace “measurements” with “estimates” because mass scattering efficiency is not measured.

Page 2 Line 14: “measurements” has been replaced with “estimates”.

Pg 3:8, Define coarse mass as “PM10-PM2.5”

This definition has been added.

Page 3 Line 9-10: “Collected PM_{10} undergoes gravimetric analysis for total particulate mass less than 10µm, allowing for the determination of coarse mass (PM_{10}-$PM_{2.5}$)”

Pg 3:5, bsp isn’t measured at all the sites. Perhaps add a line saying that bsp is measured at a subset of sites. This is stated in line 10, but it could be misunderstood here. Perhaps bsp and RH could be left off this list here and then it is clear from line 10 that they are measured at a subset of sites.

Clarification has been added to indicate that bsp and RH are measured at a subset of IMPROVE sites.

Page 3 Line 4:6: “The network offers measurements of $PM_{2.5}$ speciation, $PM_{2.5}$ and PM_{10} gravimetric mass, and collocated measurements of b_{sp} and RH at a subset of sites that we interpret to understand mass scattering efficiency.”

Pg 3:10, bsp is “reported”, not “measured” hourly.

Thank you, this has been corrected (now page 3, line 12).

Pg 3:14, It is important to consider the impacts of the truncation error for the open air nephelometer and how this can affect scattering where coarse mass is a major contributor.

To investigate the possible bias introduced by nephelometer truncation of coarse mass, the fourth panel of Figure 4 shows calculated vs. measured mass scattering efficiency in conditions dominated by coarse mass ($PM_{coarse}/PM_{10} > 0.6$). While there is a slight overestimation of mass scattering efficiency in calculated α_{sp} compared to measured α_{sp} in PM_{coarse} dominant conditions, this overestimation is more pronounced in conditions dominated by secondary inorganic and organic aerosols. It appears that on average, the bias introduced by nephelometer truncation is not as significant as the bias in the representation of SIA and OA parameters. For this reason, we focus on the representation of SIA and OA parameters.

Page 5 Line 20-22: “Although the OPTEC open air nephelometer reduces truncation error compared with other nephelometers, truncation error can be significant for coarse particles (Hand and Malm, 2007; Lowenthal and Kumar, 2006). Thus our analysis below focuses on conditions dominated by fine mode aerosols, and mechanisms affecting fine mode aerosols.”

Pg 3:16-17, Can the authors elaborate on why sea salt concentrations are not available before 2005? What parameter is being used to calculate sea salt?

IMPROVE uses the chloride ion to estimate sea salt concentrations by SS=1.8[Cl^-]. From 2000-2003, many samples at interior sites reported negative chloride concentrations. This has been associated with chloride backgrounds present on the Nylon filters used during this time period (see data advisory: http://vista.cira.colostate.edu/improve/Data/QA_QC/Advisory/da0036/da0036_chloride_loss.pdf) At the time IMPROVE data was downloaded, SS concentrations were unavailable from 2000 through 2004.

The following sentence has been added to clarify that sea-salt is not reported:

Page 3 Line 25-27: Sea salt aerosols are excluded from the analysis from 2000-2004, as reliable estimates of sea salt concentrations were unavailable during this period. We exclude coastal sites during this period, as sea salt can contribute significantly to b_{sp} in coastal conditions of high RH due to its highly hygroscopic nature (Lowenthal and Kumar, 2006).

Pg 3:20, Do the authors also apply completeness criteria for mass? How many complete years are required for this time period?

Clarification has been added regarding completeness criteria for mass. This section now reads "We use only days with coincident mass and scatter measurements, and a minimum of 23 hourly measurements per day, to reduce influence of meteorological interference. Additionally, only sites with a minimum of 90 days of measurements are included in the analysis."

Pg 3:21, Does average bsp here correspond to ambient RH conditions? Are these the average of daily values or annual values?

Average b_{sp} corresponds to ambient RH conditions, and these are the average of hourly b_{sp} values. The following clarification has been added:

Page 3 Line 31-32: "Figure 1 shows at the 28 sites used in this study the average hourly b_{sp} at ambient RH and the average 24h PM_{10} and $PM_{2.5}$ measured between 2000-2010."

Pg 4:5, Have the authors considered the influence of this multiplier on mass scattering efficiency? Comparisons of mass and bsp at dry conditions would help show that these assumptions are also appropriate and not affecting efficiencies.

Interesting idea. Although this multiplier is one of several parameters that influence modelled mass scattering efficiency in section 3.3, it does not affect the bulk of our analysis since the entirety of our analysis prior to section 3.3 does not use model output, as is explained in more detail in response to a later comment. Thus we focus on size and hygroscopicity which more directly influence mass scattering efficiency.

Unfortunately, we are unable to compare modelled and measured mass and b_{sp} in dry conditions, as IMPROVE measures b_{sp} in ambient conditions, and you mention below, the RH at which PM_{10} mass is measured is not dry.

Pg 4:10, Please note that the IMPROVE PM2.5 measurement is not a FRM measurement and after 2011 the laboratory RH varied significantly and could contribute a large bias to PM2.5 and PM10 measurements (they are not "dry"). See the data advisory at: http://vista.cira.colostate.edu/improve/Data/QA_QC/Advisory/da0035/da0035_IncreasedRH.pdf

Thank you for bringing this to our attention. Data from 2011-2015 has been removed from the analysis to address this concern. The removal of these four years of data, and the implementation of more rigorous completeness criteria for mass has resulted in slight changes in most of our plots. Most of our results have remained the same, however κ_s has increased from 0.58 to 0.61.

It should be noted that in this analysis, $PM_{2.5}$ and PM_{10} measurements are not assumed to be dry. It is assumed that PM2.5 and PM_{10} mass measurements are performed at 40% RH. Further clarification on this has been added in section 2.3.

Section 2.3 (Page 5 Line 10-12): "We define α_{sp} operationally here based on optical measurements at ambient RH, and PM measurements at controlled RH (treated as 40% RH for consistency with IMPROVE protocols prior to 2011). At 40% RH, hygroscopic components of PM_{10} will have associated water, and thus measured PM_{10} mass is not treated as dry."

Pg 4:11, What RH are these calculated at- model or measured?

Particle scatter and aerosol optical depth are calculated at modelled ambient RH. The word "modelled" has been added to this sentence for clarification.

Page 4 Line 20-22: "Particle scatter and aerosol optical depth are calculated at modelled ambient RH based on dry species mass concentrations and aerosol physical and optical properties."

Pg 4:15, Do the comparisons with the IMPROVE network correspond only to IMPROVE data from 2006 or from an average of 2000-2015? Given the yearly variability, it would more defendable to compare data and modeled values over the same time period.

Only simultaneous hourly modelled and measured mass scattering efficiencies are used in the comparison. "Coincident" and "over the same time period" have been added to the sentence for clarification:

Page 4 Line 26-28 "We simulate $PM_{10,}$ $PM_{2.5}$ and b_{sp}, allowing for the comparison of model mass scattering efficiency coincident to that measured at IMPROVE network sites over the same time period over North America."

Pg 4: Section 2.3 I have several questions regarding how mass scattering efficiencies are calculated. As mentioned before, truncation errors for the open air nephelometer can impact measured bsp (See Malm and Hand, 2007), essentially removing some (up to half) of the CM scattering – resulting in a discrepancy between scattering and PM10 mass.

To investigate the possible bias introduced by nephelometer truncation of coarse mass, the fourth panel of Figure 4 shows calculated vs. measured mass scattering efficiency in conditions dominated by coarse mass (PM_{coarse}/PM_{10} > 0.6). While there is a slight overestimation of mass scattering efficiency in calculated α_{sp} compared to measured α_{sp} in PM_{coarse} dominant conditions, this overestimation is more pronounced in conditions dominated by secondary inorganic and organic aerosols. It appears that on average, the bias introduced by nephelometer truncation is not as significant as the bias in the representation of SIA and OA parameters. For this reason, we focus on the representation of SIA and OA parameters.

Page 5 Line 20-22"Although the OPTEC open air nephelometer reduces truncation error compared with other nephelometers, truncation error can be significant for coarse particles (Hand and Malm, 2007; Lowenthal and Kumar, 2006).

Thus our analysis below focuses on conditions dominated by fine mode aerosols, and mechanisms affecting fine mode aerosols."

In addition, dividing ambient bsp by a "dry" PM10 results in an 'enhanced' mass scattering efficiency if bsp and mass don't have the same amount of associated water. PM10 is generally "dry", but as mentioned earlier, after 2011 it can contain a significant amount of water based on the uncontrolled laboratory measurement RH which has nothing to do with ambient RH. If you're comparing data only from 2006 this won't be an issue. But missing the coarse mass contribution to bsp could result in an underestimate of mass scattering efficiency depending on location because in some regions CM is a major contributor to PM10.

In section 2.3, we acknowledge that multiple definitions of mass scattering efficiency exist, and given the nature of the measurements available, we define mass scattering efficiency for this analysis as b_{sp} at ambient RH divided by gravimetric PM_{10} mass at 40% RH.

The following sentence has been added to clarify that gravimetric PM_{10} mass is not treated as dry. Page 5, Line 11-12:"At 40% RH, hygroscopic components of PM_{10} will have associated water, and thus measured PM_{10} mass is not treated as dry."

We also exclude data after 2010 when lab RH becomes variable. Page 3, Line 24-25: "We exclude data after 2010 to address concerns about variable laboratory RH for PM_{10} measurement after 2010."

It is unclear to me why IMPROVE mass is used to estimate the modeled mass scattering efficiency? This would seem to introduce more uncertainty and less consistency in the estimates, especially given the spatial resolution of the model.

This approach enables isolation of the mass scattering efficiency used in GEOS-Chem from the species concentrations. We added text to clarify the method.

Page 4 line 8-12: "The majority of our analysis focuses on the accuracy of the GEOS-Chem parameterization of mass scattering efficiency based on optical parameters given in Table A1. These default aerosol physical and optical properties are defined by the Global Aerosol Data Set (GADS) (Koepke et al., 1997), as implemented by Martin et al. (2003), with modifications to dry size distributions (Drury et al., 2010) and dust mass partitioning (Ridley et al., 2012). After evaluating and improving this parameterization, implications are examined using the full GEOS-Chem simulation in section 3.3."

It would be helpful to see a comparison of modeled and measured mass concentrations and bsp. Do the predictions of SIA and OA generally agree with the observations? Can the model accurately predict measured bsp? It seems it would be important to know the model performance of the parameters that go into estimating mass scattering efficiency before trying to tune the model results using size and hygroscopicity. While perhaps the new revised estimates are more accurate, it is hard to know whether they are just accounting for other issues within the model or the measurements. Without the basic comparisons, the comparison is less convincing.

There seems to be a misunderstanding here regarding our methods. Rather than using model output of mass scattering efficiency to refine size and hygroscopicity parameters, we calculate mass scattering efficiency using IMPROVE speciation measurements alongside aerosol physical and optical properties from the model. We then use this calculated mass scattering efficiency to refine size and hygroscopicity parameters. This removes the influence of possible biases in model output from the analysis. Thus the comparison of modeled and measured mass concentrations and b_{sp} are irrelevant.

On page 4, line 8-12 we added "The majority of our analysis focuses on the accuracy of the GEOS-Chem parameterization of mass scattering efficiency based on optical parameters given in Table A1. These default aerosol physical and optical properties are defined by the Global Aerosol Data Set (GADS) (Koepke et al., 1997), as implemented by Martin et al. (2003), with modifications to dry size distributions (Drury et al., 2010) and dust mass partitioning (Ridley et al., 2012). After evaluating and improving this parameterization, implications are examined using the full GEOS-Chem simulation in section 3.3."

GEOS-Chem model output is used in this analysis in section 3.3 only, when we investigate how the changes to size and hygroscopicity impact model output.

Pg 5:4, What is "v" as the kappa subscript refer to?

Thanks for bringing this to our attention, the subscript "v" has been removed from equation 5 (formerly equation 4) and page 6, line 7.

Pg 5:20, Include "annual" before "average".

The average mass scattering efficiencies described here are averages over the entire sampling period at each IMPROVE site, not annual averages. A sentence has been added to section 2.3 describing how average mass scattering efficiency is calculated for each site.

Page 5 Line16-19: "To reduce the impacts of meteorological variation on the comparison of measured and calculated mass scattering efficiency, we perform averages of hourly $b_{sp,calc}$, $b_{sp,meas}$, and PM_{10} over the entire sampling period at each IMPROVE site *i*. Eq. (3) is then used to obtain average calculated and measured mass scattering efficiency at each site.

$$\alpha_{sp,avg,i} = \frac{b_{sp,avg,i}}{PM_{10,avg,i}} \qquad (3)$$"

Page 6 Line 12-13: "Each point represents the average α_{sp} over the entire sampling period at each IMPROVE site."

Pg 5:22, It would help to at least mention that the figure also includes revised estimates that will be introduced later, otherwise the figures appear to be referred to out of numeric order (figure 3 is discussed before figure 2, right side- etc.).

This has been added to page 6 line 15: "(The right panel of Figure 2 is discussed below.)"

Pg 6:1, Is the PM2.5 here referring to observations or model estimates?

The $PM_{2.5}$ is referring to observations. The word "measured" has been added before $PM_{2.5}$ to clarify.

Page 6 Line 26-28: Figure 4 shows in blue average measured vs calculated α_{sp} using default optical tables for conditions where measured $PM_{2.5}$ is dominated (>60%) by secondary inorganic aerosol, organic aerosol and fine dust, as well conditions where PM_{10} is dominated (>60%) by PM_{coarse} (PM_{10}-$PM_{2.5}$).

Pg 6:1, Add "fine" before "dust"

This change has been made. The sentence now reads:

Page 6 Line 26-28: Figure 4 shows in blue average measured vs calculated α_{sp} using default optical tables for conditions where measured $PM_{2.5}$ is dominated (>60%) by secondary inorganic aerosol, organic aerosol and fine dust, as well conditions where PM_{10} is dominated (>60%) by PM_{coarse} (PM_{10}-$PM_{2.5}$)

Pg 6:12, Can the authors reconcile studies that demonstrate that even at low RH particles will still have water associated with them? (e.g., Santarpia et al., 2004, 2005; Carrico et al., 2000, 2003, 2005; ten Brink et al., 2006; Malm and Day, 2001; Malm et al., 2003, 2005; Xu et al., 2002; Im et al., 2001; Eldering et al., 2002).

While we later inhibit hygroscopic growth of SIA below 35% RH, we reconcile this by allowing hygroscopic growth of organics at low RH.

Pg 8:20, The authors have seemingly tuned their model to the parameters that give the closest agreement with observations so it isn't surprising that the revised estimates agree more closely. However, they don't comment on why the model inherently had too large of sizes. Have other studies also observed this? Is it consistent with size distributions measured at surface sites? Given some of the issues with observations mentioned earlier, it would be important to understand whether the model adjustments are just accounting for some of the measurement biases. This could be partly answered if comparisons of modeled and measured mass concentrations and bsp were performed.

The initial aerosol sizes used in the current version of GEOS-Chem were based on summertime aerosol measurements (Drury et al., 2011), when aerosols are larger. This serves as a reasonable explanation for why the model inherently has too large of sizes in seasons other than summer. The following sentence has been added for clarification:

Page 8 Line 28-29: "This annual radius is smaller than the GEOS-Chem default sizes of SIA and OA that were informed by summertime measurements alone (Drury et al., 2010)."

Available aerosol size distribution measurements at surface sites in North America are mostly limited to small particle size ranges, and therefore do not include particles large enough to be useful for comparisons in our study. We have however included the following sentence to compare our seasonal aerosol size results to measurements performed by Levin et al. in 2006:

Page 8 Line 26-27: "The spring and summer radii are consistent with accumulation mode size distribution measurements performed by Levin et al. (2009) in the spring and summer of 2006."

As previously stated, modelled mass concentrations have not been used in this analysis and are thus irrelevant for this discussion.

Pg 9:18, Mass scattering efficiencies of 10-12 m2/g are exceptionally high unless they correspond to enhanced scattering efficiencies with higher RH bsp and dry mass. Providing the RH that these values correspond to is important.

As the definition of mass scattering efficiency used in this study is $b_{sp\ (ambient\ RH)}$ / $PM_{10\ (40\%\ RH)}$, mass scattering efficiencies will be enhanced in conditions of high humidity. The following sentence has been added:

Page 10 Line 22-23: "The elevated mass scattering efficiencies in the northwest can be attributed in part to the high average RH in this region of 83%."

Pg 11:14, Again it would be helpful to show a comparison of measured and modeled bsp and of mass separately.

Again, the GEOS-Chem mass scattering efficiency parameterization is not calculated from the ratio of modelled mass to b_{sp}. We have added the following text to clarify.

Page 4 Line 8-12: "The majority of our analysis focuses on the accuracy of the GEOS-Chem parameterization of mass scattering efficiency based on optical parameters given in Table A1. These default aerosol physical and optical properties are defined by the Global Aerosol Data Set (GADS) (Koepke et al., 1997), as implemented by Martin et al. (2003), with modifications to dry size distributions (Drury et al., 2010) and dust mass partitioning (Ridley et al., 2012). After evaluating and improving this parameterization, implications are examined using the full GEOS-Chem simulation in section 3.3."

Page 4 Line 22-24: "The GEOS-Chem aerosol simulation has been extensively evaluated with observations of mass (van Donkelaar et al., 2015; Li et al., 2016), composition (Kim et al., 2015; Marais et al., 2016; Philip et al., 2014a), and scatter (Drury et al., 2010)."

Pg 12:4, Again, see the earlier advisory. IMPROVE PM2.5 and PM10 measurements are not FRM.

Thank you, this has been addressed by removing data from 2011-2015 from the analysis.

Pg 12:8, Why is it necessary to partition IMPROVE OM? Unless I have missed something, hygroscopic calculations for IMPROVE mass weren't done as part of this paper?

In order to calculate α_{sp} from IMPROVE speciation measurements using Eq. A2:

$$\alpha_{sp} = \frac{B_{sp}}{PM_{10}} = \frac{\sum_{species,i} \frac{\frac{3}{4} * \left(\frac{R_{w,i}}{R_{d,i}}\right)^2 * \frac{M_{d,i}}{PM_{10}} * Q_{w,i} * SSA_{w,i}}{\rho_{d,i} * R_{d,i}}}{PM_{10}} \qquad (A2)$$

we need to know the dry effective radius (R_d) and the dry mass density ρ_d, as well as the wet effective radius (R_w), the wet extinction efficiency (Q_w), and the wet single scattering albedo (SSA_w) of a given species. In order to calculate these wet parameters, we need to know the water uptake by a given species at a given RH value. It is therefore necessary to perform hygroscopic calculations for IMPROVE speciation.

We have added “to enable isolation of mass scattering efficiency in our comparisons” to page 13, line 11-12:

“The GEOS-Chem model partitions OM into hydrophilic and hydrophobic fractions, so the same is done for OM measured by IMPROVE to enable isolation of mass scattering efficiency in our comparisons.”

Figures:

Pg 19:4, Figure 1, Provide the wavelength and RH (or state ambient) for bsp. The sentence starting with “overlaying circles” seems redundant.

These details have been added, and “overlaying circles” has been removed.

Page 22: “Figure 1: Map of IMPROVE sites with collocated scatter (b_{sp}) at 550 nm and ambient relative humidity, PM_{10} and $PM_{2.5}$ measurements in North America between 2000-2010.”

Pg 20, Figure 2, please include the years included in the comparison, and the wavelength corresponding to the efficiency. It would help to also denote the parts of the figure as well.

The caption of Figure 2 has been changed to include the wavelength of mass scattering efficiency and the years included in the comparison.

Page 23: “Figure 2: Average measured vs calculated α_{sp} at 550 nm at IMPROVE sites between 2000-2010 using GEOS-Chem default optical tables and revised optical tables. The colour of each point corresponds to the average relative humidity at the site. The 1:1 line is black. Slope, offset and correlation coefficient are inset.”

Pg 20, Figure 3: Similar comment regarding wavelength as other figures (this is helpful for readers if they are scanning figures and don’t have to dig through the text for this information). Please include the years this comparison was made over. Also comment on “default” and “revised”.

The caption of Figure 3 has been changed to include the wavelength of mass scattering efficiency and the years included in the comparison. “Default” and “revised” are noted in the caption.

Page 23: “Figure 3: Average measured versus calculated α_{sp} at 550 nm at IMPROVE sites between 2000-2010 using GEOS-Chem default and revised optical tables (Table A1) for measurements taken in 0-35 % RH, 35-65 % RH and 65-95 % RH conditions. The 1:1 line is black. Slope, offset and correlation coefficient are inset.”

Pg 21, Figure 4: Include wavelength. Define SIA, OA, PMcoarse. Are these delineations based on modeled or measured composition measurements? Please state in caption. Also include RH ranges (ambient?) and years of comparison.

Wavelength, as well as definitions of SIA, OA and PM_{coarse}, and years of comparison have been incorporated into the caption of Figure 4. The delineations are based on IMPROVE composition measurements- this is now stated in the caption.

Mass scattering efficiency is defined for this analysis as b_{sp} (ambient RH) / PM_{10} (40 % RH). It is therefore not appropriate to state an RH range. This definition is used throughout the entire analysis.

Page 24: “Figure 4: Average measured versus calculated α_{sp} (550 nm) at IMPROVE sites between 2000-2010 using GEOS-Chem default and revised optical tables for measurements taken in conditions dominated by secondary inorganic aerosols (SIA), organic aerosols (OA), fine dust, and PM_{coarse} (PM_{10}-$PM_{2.5}$). The 1:1 line is black. Slope, offset, and correlation coefficient are inset.”

Pg 21, Figure 5: Please include wavelength. What kappa was used for OC and SIA?

The wavelength has been added to the caption. For this figure, water uptake for OA and SIA was calculated using GEOS-Chem default hygroscopic growth factors. To clarify, a sentence has been added.

Page 7 Line 13-14: Water uptake at 80% RH for OA and SIA is calculated using default hygroscopic growth factors from GEOS-Chem.

Pg 22, Figure 6: Please include wavelength and years of comparison.

The caption of Figure 6 has been changed to include the wavelength of mass scattering efficiency and the years included in the comparison.

Page 25: “Figure 6: Average measured versus calculated a_{sp} (550 nm) at IMPROVE sites between 2000-2010 using GEOS-Chem default and revised optical tables for measurements taken in dry conditions (RH<35 %) in winter, spring, summer and fall. The 1:1 line is black. Slope, offset and correlation coefficient are inset.”

Pg 23, Figure 8: Please define kappa,s and kappa,o.

κ_o and κ_s have been defined in the caption of Figure 8.

Page 26: “Figure 8: Slope of measured vs. calculated α_{sp} plot as a function of the κ of secondary inorganic aerosols (κ_S, left) and the κ of organic aerosols (κ_O, right). The line slope=1 is shown in black. κ_s and κ_o values for which slope=1 are inset.”

Pg23, Figure 9: Please define SIA and OA. “Hygroscopic” has a typo.

This typo has been fixed, and SIA and OA have been defined in the caption of figure 9.

Page 26 Line 5: “Hygroscopic growth factor curves for secondary inorganic aerosols (SIA, left) and organic aerosols (OA, right).”

Pg 24, Figure 10: Define SIA and OA.

For clarification, “SIA and OA” has been removed and replaced with “secondary inorganic and organic aerosols” in the caption of Figure 10.

Page 27 “Figure 10: Average relative and absolute change in GEOS-Chem mass scattering efficiency over North America for the year 2006 after implementing revised optical tables for secondary inorganic and organic aerosols.”

Pg 25, Figure 11: Please provide wavelength and RH (ambient?), define SIA and OA. This color table makes it hard to see the sites in the Southwest.

The wavelength has been added to the caption, and “SIA and OA” has been replaced with “secondary inorganic and organic aerosols”.

Again, RH is ambient for b_{sp}, but 40% for PM_{10}, so it is not appropriate to provide an RH for mass scattering efficiency.

The colormap has been changed for this plot.

Page 28: “Figure 11: GEOS-Chem annual average mass scattering efficiency (at 550 nm) for the year 2006 using default and revised size and hygroscopicity for secondary inorganic and organic aerosols.”

Pg 26: Figure 12: Please provide wavelength and RH (ambient?)

The wavelength has been added to the caption. Again, RH is ambient for b_{sp}, but 40% for PM_{10}, so it is not appropriate to provide an RH for mass scattering efficiency.

Page 29: “Figure 12: Coincident simulated versus measured average mass scattering efficiency at 550 nm for the year 2006, using default and revised optical tables.”

Pg 28, Figure B2: This color table makes it hard to see the comparisons.

The colormap has been changed for this plot.

Pg 30, Table A1, Define SIA and OA, kappa,s and kappa,o (use similar subscripts as SIA and OA?)

SIA, OA, κ_s, and κ_o have been defined in the caption of Table A1.

Page 33 Line 21-23: “Table A1: Default and revised aerosol size and optical properties for secondary inorganic aerosols (SIA) and organic aerosols (OA) at 550 nm at 8 relative humidity values. Columns indicate geometric mean radius (r_g), effective radius (r_{eff}), extinction efficiency (Q), and single scattering albedo (SSA). κ_s and κ_o represent the hygroscopic growth parameters for SIA and OA, respectively.”

Reviewer: 2

The paper studies an important topic for chemistry transport modeling the mass scattering efficiency that affects the conversion from aerosol mass to aerosol extinction and ultimately AOD. Mass scattering efficiency data from IMPROVE is used to constrain a global CTM (GEOS-Chem, GC). It is found that geometric mean radiuses for both dry secondary inorganic and organic aerosols in original GC configuration need to be decreased, and also the aerosol hygroscopicity curve needs to be adjusted to be less hygroscopic. Overall, the paper should be considered for publication after a major revision (and possibly another review).

General comments

1) There are lots of averaging done in the data analysis. For example, the captions for Figures 2, 3, 4, and 6 all start with the word 'average', But, how averaging is done is not described in the method section. In addition, how much is the standard deviation in the average?

Clarifications regarding how averaging is done in the analysis have been added and are discussed in detail below. The average mass scattering efficiency at each site is calculated by dividing the average scattering coefficient by the average mass concentration at each site. Variations in these two parameters occur over the sampling period due to variations in relative humidity, composition and size distribution.

2) only R and best fit are shown in all scatter plots. How about RMSE and bias?

RMSE and bias have been added to Figures 2, 3, 4, 6, 12 and B.3.

3) some discussion of uncertainties here are needed. what are the uncertainties in the measurements of scattering coefficient bsp and surface PM2.5? Likewise, do GEOS fields have any systematic bias in simulating RH?

A paragraph discussing uncertainties in PM and b_{sp} have been added to section 2.1.

Page 3 Line 17-22: "The IMPROVE network collects collocated samples at a subset of sites, which can provide insight into precision errors associated with the measurements of major species. Hyslop and White (2008) and Solomon et al. (2014) found mean collocated precision errors ranging from 6-11% for particulate mass measured by IMPROVE. Typical uncertainties in IMPROVE b_{sp} measurements are in the range of 5-15% (Gebhart et al., 2001). Due to nephelometer truncation errors, uncertainties in measured b_{sp} increase as particle size distributions increase, and coarse particle scattering can be underestimated (Molenar, 1997)."

Our analysis is largely independent of GEOS RH since most of our analysis uses IMPROVE RH. We clarified on page 4:

Page 4 Line 8-12: "The majority of our analysis focuses on the accuracy of the GEOS-Chem parameterization of mass scattering efficiency based on optical parameters given in Table A1. These default aerosol physical and optical properties are defined by the Global Aerosol Data Set (GADS) (Koepke et al., 1997), as implemented by Martin et al. (2003), with modifications to dry size distributions (Drury et al., 2010) and dust mass partitioning (Ridley et al., 2012). After evaluating and improving this parameterization, implications are examined using the full GEOS-Chem simulation in section 3.3."

Nonetheless we have added a citation with evaluation of GEOS RH for the interested reader (Gelaro et al., 2017).

Specific comments

Pg 4L:10. If IMPROVE PM2.5 is analyzed at 30-50% RH, there will be aerosol water in the aerosol mass measured by IMPROVE. What is the uncertainty here if we assume these are dry particle mass and used in the scattering efficiency calculation? Some consistence is needed or at least discussed between how PM2.5 dry mass is computed in GC vs. how aerosol optics (aerosol hygroscopic growth) are treated in GC. Later in the analysis, the cut off of RH is 35% to be considered as dry (solid) aerosol. Why not 40% as for dry PM2.5?

At 40% RH, we do not assume that $PM_{2.5}$ and PM_{10} mass are dry. The definition of mass scattering efficiency used in our analysis acknowledges this. A line has been added for clarification in section 2.3:

Page 5 Line 11-12: “At 40% RH, hygroscopic components of PM_{10} will have associated water, and thus measured PM_{10} mass is not considered to be dry.”

When we simulate mass scattering efficiency in GEOS-Chem in section 3.3, we use the same definition of mass scattering efficiency, with PM_{10} mass at 40% RH in the denominator.

A discussion regarding how aerosol hygroscopic growth is treated in GEOS-Chem can be found on page 9 line 12-18, and GEOS-Chem hygroscopic growth of SIA and OA are shown in Figure 9.

Pg 4:23. Effectively, b_sp is averaged each day, and then daily averages of b_sp is used together with daily PM2.5 to compute scattering efficiency. How annual average of mass scattering efficiency is computed? How the averages are computed for RH in different ranges or for different compositions (e.g., dust dominated, SIA dominated, etc.)? RH does have a strong diurnal variation.

Clarifications regarding how averages are computed overall, for different RH ranges, and for different compositions have been added.

Page 5 Line 16-19: “To reduce the impacts of meteorological variation on the comparison of measured and calculated mass scattering efficiency, we perform averages of hourly $b_{sp,calc}$, $b_{sp,meas}$, and PM_{10} over the entire sampling period at each IMPROVE site *i*. Eq. (3) is then used to obtain average calculated and measured mass scattering efficiency at each site.

$$\alpha_{sp,avg,i} = \frac{b_{sp,avg,i}}{PM_{10,avg,i}} \qquad (3)”$$

Page 6, Line 17-19 “The IMPROVE data is divided among the RH groupings using IMPROVE measurements of hourly RH. Within each grouping, average calculated and measured mass scattering efficiencies are obtained for each site using Eq. (3).”

Page 6, Line 24-26: “Using IMPROVE measurements of 24 hr $PM_{2.5}$ mass and speciation and PM_{10} mass, the IMPROVE data is grouped based on dominant aerosol type. Within each group, average calculated and measured mass scattering efficiency is obtained for each site using Eq. (3).”

Pg 6:20-24. The uncertainty of aerosol mass scattering efficiency can also come from the particle composition which essentially affect the particle hygroscopic growth factor, or particle size and density. the scattering efficiency of sulfuric acid vs. ammonium sulfate can be different even for the same size distribution at dry conditions. See "Table 1 in Sensitivity of sulfate direct climate forcing to the hysteresis of particle phase transitions, JGR, 2008". The mass scattering efficiency can also be affected by the mixing state of the particle. The analysis here needs to discuss these uncertainties before focusing on particle size.

We added the following text:

Page 2 Line 4-5: "Mass scattering efficiency is a complex function of aerosol size, composition, hygroscopicity and mixing state (Hand and Malm, 2007; Malm and Kreidenweis, 1997; White, 1986)"

Pg 7:2-3. What is the seasonality of aerosol size distribution?

The seasonality of the aerosol size distribution is described in the previous paragraph, now page 7, line 26-27: "Aerosol surface area and volume distributions fluctuate seasonally in the North Eastern U.S., with summer maxima and winter minima (Stanier et al., 2004)."

Pg 7:13-15. Martin et al's paper showed there can be aerosols in solid phase in RH larger than 40%. The phase transition depends on RH history of the particle, not just RH itself. Could this explain the part of overestimation in GC mass scattering efficiency? What is the fraction of solid SIA particles in U.S.? this paper might be helpful – "global distribution of solid and aqueous sulfate aerosols . . ., JGR, 2008".

The following sentence has been added to acknowledge the possible importance of particle RH history.

Page 11 Line 7: Representation of particle RH history may also be important (Wang et al., 2008).

Pg 8:5. What is r_sp used in figure 8?

The new dry radius of 0.058 μm from section 3.2.2 is used in figure 8. The following sentence has been added to the end of section 3.2.2. to provide clarification:

Page 9 Line 2-3: "For the remainder of the analysis, this new dry radius of 0.058 μm is implemented for SIA and OA."

Pg 11:20. Again, it is the composition that regulates the growth factor and density. The real index of refraction also has the effect on scattering efficiency. In addition, the paper didn't mention effective variance at all. Is it important? References are needed here to support the statements.

A sentence has been revised to note the role of composition.

Page 14 Line 10-12: "In summary, the revised optical properties developed for North America slightly improve the representation of AOD at the global scale, despite the large influence of other factors (e.g. ambient aerosol concentrations and composition) upon AOD."

A sentence has been added on effective variance.

Page 8 Line 19-20: “Effective variance may also be important (Chin et al., 2002) but given sufficient information to simultaneously constrain size and variance, we focus on size.

Pg 13:7-8. The aerosol concentration is the same here for both figures. It is likely that the improvement with new optics is within the range of inter-annual variability of alpha_sp itself? It will be more convincing that the validation is done using other years data (say 2007 or 2008).

To repeat the analysis for additional years would be a substantive undertaking. This has been added as a suggestion for future work (page 12, line 3).

Figure 5. Caption. Is aerosol effective radius shown for dry (solid) or wet particles?

Aerosol effective radius is shown for wet particles, clarification has been added to the caption of Figure 5:

Page 24: “Figure 5: Mass scattering efficiency (α_{sp}) at 550 nm as a function of aerosol wet effective radius for organic aerosol and secondary inorganic aerosol.”

Figure 9. The GADS assume sulfate as 75% H2SO4, which often has the largest hygroscopic growth. For lab data, please provide reference. Also, lab data clearly shows that ammonium sulfate particles can be in solid phase in range of RH between 40-80%, which may explain why GC has an overestimation in scattering efficiency. How large is the uncertainty in assuming that all SIA are aqueous in RH of 40-80%? If particles are in solid phase in upper troposphere (as models suggest), the large improvement in surface with new optics may not be reflected in the AOD comparison.

The reference has been added for the lab data in the caption of Figure 9.

To address the possible importance of RH history, the following sentence has been added.

Page 11 Line 7: “Representation of particle RH history may also be important (Wang et al., 2008)”

Figure 12. add RMSE, and also, how the spectral AOD (or Angstrom exponent) is compared against AERONET? This can be an interesting test for new optics that is a result of adjusting particle size. Particle size affects both scattering efficiency as well as the spectral AOD slope. Ideally, the new optics should provide an overall improvements for the model.

RMSE and bias have been added. Aeronet spectral AOD, or Angstrom exponent, largely reflect the ratio of coarse to fine mass and is beyond the scope of this analysis.

Interpretation of Measured Aerosol Mass Scattering Efficiency Over North America Using a Chemical Transport Model

Robyn N. C. Latimer[1*], Randall V. Martin[1,2*]

[1]Department of Physics and Atmospheric Science, Dalhousie University, Halifax, B3H 4R2
[2]Harvard-Smithsonian Center for Astrophysics, Cambridge, MA 02138, USA

Correspondence to: Robyn Latimer (robyn.latimer93@gmail.ca) and Randall Martin (randall.martin@dal.ca)

Abstract. Aerosol mass scattering efficiency affects climate forcing calculations, atmospheric visibility, and the interpretation of satellite observations of aerosol optical depth. We evaluated the representation of aerosol mass scattering efficiency (α_{sp}) in the GEOS-Chem chemical transport model over North America using collocated measurements of aerosol scatter and mass from IMPROVE network sites between 2000-2010. We found a positive bias in mass scattering efficiency given current assumptions of aerosol size distributions and particle hygroscopicity in the model. We found that overestimation of mass scattering efficiency was most significant in dry (RH<35%) and midrange humidity (35%<RH<65%) conditions, with biases of 82% and 40%, respectively. To address these biases, we investigated assumptions surrounding the two largest contributors to fine aerosol mass, organic (OA) and secondary inorganic aerosols (SIA). Inhibiting hygroscopic growth of SIA below 35% RH and decreasing the dry geometric mean radius, from 0.069 μm for SIA and 0.073 μm for OA to 0.058 μm for both aerosol types, significantly decreased the overall bias observed at IMPROVE sites in dry conditions from 82% to 9%. Implementation of a widely used alternative representation of hygroscopic growth following κ-Kohler theory for secondary inorganic (hygroscopicity parameter κ=0.61) and organic (κ=0.10) aerosols eliminated the remaining overall bias in α_{sp}. Incorporating these changes in aerosol size and hygroscopicity into the GEOS-Chem model resulted in an increase of 16% in simulated annual average α_{sp} over North America, with larger increases of 25% to 45% in northern regions with high RH and hygroscopic aerosol fractions, and decreases in α_{sp} up to 15% in the southwestern U.S. where RH is low.

Deleted: 5
Deleted: 7
Deleted: 38
Deleted: 7
Deleted: 13
Deleted: 58
Deleted: S
Deleted: increased by 12%
Deleted: 0
Deleted: 0

1. Introduction

The interaction of atmospheric aerosols with radiation has substantial implications for the direct radiative effects of atmospheric aerosols, atmospheric visibility, and satellite retrievals of aerosol optical properties. The direct radiative effects of aerosols remain a major source of uncertainty in radiative forcing (Myhre et al., 2013). Atmospheric visibility affects the appearance of landscape features, which is of particular concern in national parks and wilderness areas (Malm et al., 1994)**.** Gaining insight into the concentration and composition of atmospheric aerosols via interpretation of satellite retrievals of aerosol optical depth (AOD) also relies heavily on an understanding of the interaction of aerosols with radiation (Kahn et al., 2005). Analysis of collocated measurements of aerosol scatter, mass, and composition could offer valuable insight into aerosol optical properties.

Mass scattering efficiency is a complex function of aerosol size, composition, hygroscopicity and mixing state (Hand and Malm, 2007; Malm and Kreidenweis, 1997; White, 1986). Current chemical transport models and global circulation models often calculate atmospheric extinction due to aerosols from speciated aerosol mass concentrations using a composition and size dependent mass extinction efficiency (α_{ext}, m^2 g^{-1}). Many of these models use aerosol optical and physical properties defined by the Global Aerosol Data Set (GADS), compiled from measurements and models from 1970 to 1995 (Koepke et al., 1997). The subsequent expansion in long term aerosol monitoring offers an exciting possibility to further improve model representation of aerosol physical and optical properties. The Interagency Monitoring of Protected Visual Environments (IMPROVE) network offers long-term collocated measurements since 1987 of particle scatter (b_{sp}), relative humidity (RH), particulate mass concentrations less than 10 µm (PM$_{10}$) and less than 2.5 µm (PM$_{2.5}$), as well as PM$_{2.5}$ chemical composition at sites across the United States and Canada (Malm et al., 1994; Malm et al., 2004). These collocated measurements provide direct estimates of mass scattering efficiency (α_{sp}) across North America that are useful to evaluate and improve the mass scattering efficiency currently used in models.

Deleted: growth

Deleted: fine

Deleted: mass

Deleted: measurements

Several prior studies have analysed mass scattering efficiencies. Hand et al. (2007) performed an extensive review that examined and compared mass scattering efficiencies calculated from ground based measurements from approximately 60 mostly short-term studies from 1990 to 2007. In this review, the importance of long term measurements was emphasized. Malm & Hand (2007) applied IMPROVE network data between 1987-2003 to evaluate mass scattering efficiency of organic and inorganic aerosols at 21 IMPROVE sites. A couple more recent examples of short term studies of mass scattering efficiency are Titos et al. (2012) and Tao et al. (2014). Many other long-term multi-site studies have investigated aerosol optical properties (e.g. Andrews et al., 2011; Coen et al., 2013; Pandolfi et al., 2017), but few include measurements of aerosol mass concentrations and therefore do not provide information on mass scattering efficiencies. Our study builds upon previous studies of mass scattering efficiency by reducing initial assumptions regarding size and hygroscopicity of inorganic and organic aerosols and by using measurements of particle speciation, mass and scatter to inform the representation of these properties. We interpret long term measurement data to obtain a representation of mass scattering efficiency that can be used across an array of conditions and locations to facilitate incorporation into chemical transport models.

Deleted: analyzed

Here we interpret collocated measurements of PM$_{2.5}$, PM$_{10}$, b_{sp} and RH from the IMPROVE network to understand factors affecting the representation of mass scattering efficiency. Section 2 provides a description of IMPROVE network measurements, of the GEOS-Chem chemical transport model, and of an alternate aerosol hygroscopic growth scheme. In Section 3, we present an analysis of the current representation of mass scattering efficiency in the GEOS-Chem model, and identify changes that improve the consistency with observations. The impact of these changes on GEOS-Chem simulated mass scattering efficiency, as well as on agreement between the GEOS-Chem model and observations from the IMPROVE network are described in section 4.

2. Methods

2.1 IMPROVE network measurements

The IMPROVE network (Malm et al., 1994) is a long-term monitoring program established in 1987 to monitor visibility trends in national parks and wilderness areas in the United States. The network offers measurements of $PM_{2.5}$ speciation, $PM_{2.5}$ and PM_{10} gravimetric mass, and collocated measurements of b_{sp} and RH at a subset of sites that we interpret to understand mass scattering efficiency.

The IMPROVE particle sampler collects $PM_{2.5}$ and PM_{10} on filters. Sampling occurs over a 24h period every third day. Collected $PM_{2.5}$ is analyzed for fine gravimetric mass, elemental concentrations (including Al, Si, Ca, Fe, Ti), ions (SO_4^{2-}, NO_3-, NO_2^-, Cl^-), and organic and elemental carbon. Collected PM_{10} undergoes gravimetric analysis for total particulate mass less than 10 µm, allowing for the determination of coarse mass (PM_{10}-$PM_{2.5}$) (Malm et al., 1994).

Particle scatter (b_{sp}) is measured at 550 nm at a subset of IMPROVE sites using OPTEC NGN-2 open air integrating nephelometers (Malm et al., 1994; Malm and Hand, 2007; Molenar, 1997). b_{sp} is reported hourly at ambient air temperature and relative humidity; all three parameters are recorded. We filter b_{sp} data to exclude measurements likely affected by meteorological interference such as fog. These conditions include an RH threshold of 95%, a maximum b_{sp} threshold of 5000 Mm^{-1} and an hourly rate of change threshold for b_{sp} of 50 Mm^{-1}, following IMPROVE filtering protocols (IMPROVE, 2004).

The IMPROVE network collects collocated samples at a subset of sites, which can provide insight into precision errors associated with the measurements of major species. Hyslop and White (2008) and Solomon et al. (2014) found mean collocated precision errors ranging from 6-11% for particulate mass measured by IMPROVE. Typical uncertainties in IMPROVE b_{sp} measurements are in the range of 5-15% (Gebhart et al., 2001). Due to nephelometer truncation errors, uncertainties in measured b_{sp} increase as particle size distributions increase, and coarse particle scattering can be underestimated (Molenar, 1997).

For this study, we select sites where fine aerosol mass and speciation measurements are collocated with IMPROVE nephelometers between 2000-2010. We exclude data after 2010 to address concerns about variable laboratory RH for PM_{10} measurement after 2010. Sea salt aerosols are excluded from the analysis from 2000-2004, as reliable estimates of sea salt concentrations were not reported during this period. We exclude coastal sites during this period, as sea salt can contribute significantly to b_{sp} in coastal conditions of high RH due to its highly hygroscopic nature (Lowenthal and Kumar, 2006). We use only days with coincident mass and scatter measurements, and a minimum of 23 hourly measurements per day, to reduce influence of meteorological interference. Additionally, only sites with a minimum of 90 days of measurements are included in the analysis.

Figure 1 shows at the 28 sites used in this study the average hourly b_{sp} at ambient RH and the average 24h PM_{10} and $PM_{2.5}$ measured between 2000-2010. Measured b_{sp} values vary by a factor of 7 with scatter below 20 Mm^{-1} across the southwest U.S., and scatter above 50 Mm^{-1} across the southeast U.S. Measured PM_{10} concentrations vary by a factor of 3

Deleted: collocated

Deleted: coarse mass

Deleted: measured

Deleted: (

Deleted: ,

Deleted: ;

Deleted: ,

Deleted:

Deleted:

Deleted: 5

Deleted: We exclude

Deleted: between 2000-2005

Deleted: since reliable estimates of sea salt concentrations were unavailable prior to 2005, and

Deleted: since

Deleted: . Additionally, only days with

Deleted: are used

Deleted: 30

Deleted: ,

Deleted: 5

with values below 6 μg m^{-3} in the west to above 14 μg m^{-3} in the southeast. Measured $PM_{2.5}$ concentrations also vary by a factor of 3, with values below 3 μg m^{-3} in the west to above 9 μg m^{-3} in the southeast.

2.2 GEOS-Chem simulation

We simulate hourly $PM_{2.5}$ and PM_{10} mass concentrations and particle scatter using the global chemical transport model GEOS-Chem (version 11.01, http://geos-chem.org). The GEOS-Chem model is driven by assimilated meteorology from the Goddard Earth Observation System (GEOS MERRA-2, (Gelaro et al., 2017) of the NASA Global Modeling and Assimilation Office (GMAO). Our simulation for North America is conducted at 2° x 2.5° resolution over 47 vertical levels.

Deleted:)

The majority of our analysis focuses on the accuracy of the GEOS-Chem parameterization of mass scattering efficiency based on optical parameters given in Table A1. These default aerosol physical and optical properties are defined by the Global Aerosol Data Set (GADS) (Koepke et al., 1997), as implemented by Martin et al. (2003), with modifications to dry size distributions (Drury et al., 2010) and dust mass partitioning (Ridley et al., 2012). After evaluating and improving this parameterization, implications are examined using the full GEOS-Chem simulation in section 3.3.

GEOS-Chem simulates detailed aerosol-oxidant chemistry (Bey et al., 2001; Park et al., 2004). The aerosol simulation includes the sulfate-nitrate-ammonium system (Park et al., 2004), primary (Park et al., 2003; Wang et al., 2014) and secondary (Pye et al., 2010) carbonaceous aerosols, mineral dust (Fairlie et al., 2007; Fairlie et al., 2010; Zhang et al., 2013) and sea salt (Jaeglé et al., 2011). Organic matter (OM) is estimated from primary organic carbon (OC) using spatially and seasonally varying OM/OC ratios at 0.1° x 0.1° resolution (Philip et al., 2014b). The thermodynamic equilibrium model ISORROPIA-II (Fountoukis and Nenes, 2007), implemented by Pye et al. (2009), is used to calculate gas-aerosol partitioning. Total PM_{10} is calculated following van Donkelaar et al. (2010), but at 40% RH here for consistency with the IMPROVE network gravimetric analysis in the range of 30-50% RH (Solomon et al., 2014). Particle scatter and aerosol optical depth are calculated at modelled ambient RH based on dry species mass concentrations and aerosol physical and optical properties. The GEOS-Chem aerosol simulation has been extensively evaluated with observations of mass (van Donkelaar et al., 2015; Li et al., 2016), composition (Achakulwisut et al., 2017; Kim et al., 2015; Marais et al., 2016; Philip et al., 2014a; Ridley et al., 2017; Zhang et al., 2013), and scatter (Drury et al., 2010).

Deleted: Aerosol physical and optical properties are defined by the Global Aerosol Data Set (GADS) (Koepke et al., 1997), as implemented by Martin et al. (2003), with modifications to dry size distributions (Drury et al., 2010) and dust mass partitioning (Ridley et al., 2012). Default optical parameters are given in Table A1.

Deleted: $_{2.5}$

We conduct a simulation for the year 2006, to represent the period of greatest measurement density of collocated b_{sp} and PM sites over North America. We archive model fields every hour over North America. We simulate $PM_{10,}$ $PM_{2.5}$ and b_{sp}, allowing for the comparison of model mass scattering efficiency coincident with that measured at IMPROVE network sites over the same time period over North America.

Deleted: to

2.3 Determining mass scattering efficiciency (α_{sp})

One method of determining mass scattering efficiencies from measurements involves b_{sp} measurements and particle mass concentration measurements (M_{meas}). Mass scattering efficiency of a given aerosol population can be defined as the ratio of particle scatter to mass.

$$\alpha_{sp,meas} = \frac{b_{sp,meas}}{M_{meas}} \quad (1)$$

Hourly mass scattering efficiencies are determined using collocated measurements of b_{sp} and mass concentrations from the IMPROVE network, treating IMPROVE mass concentrations as constant over each 24h sampling period. Total scatter is typically dominated by fine mode aerosols, but in certain conditions coarse dust can also make a significant contribution (White et al., 1994). Thus, measured PM_{10} mass is used in the denominator of Eq. (1).

Multiple definitions of α_{sp} exist. We define α_{sp} operationally here based on optical measurements at ambient RH, and PM measurements at controlled RH (treated as 40% RH for consistency with IMPROVE protocols prior to 2011). At 40% RH, hygroscopic components of PM_{10} will have associated water, and thus measured PM_{10} mass is not treated as dry. We compare these measured α_{sp} with calculated α_{sp} based on species specific mass scattering efficiencies ($\alpha_{GC,j}$) used in GEOS-Chem, constrained with mass concentrations (M_j) and PM_{10} mass measured by IMPROVE.

$$\alpha_{sp,calc} = \frac{b_{sp,calc}}{PM_{10,meas}} = \frac{\sum_j \alpha_{GC,j} M_j}{PM_{10,meas}} \quad (2)$$

To reduce the impacts of meteorological variation on the comparison of measured and calculated mass scattering efficiency, we perform averages of hourly $b_{sp,calc}$, $b_{sp,meas}$, and PM_{10} over the entire sampling period at each IMPROVE site *i*. Eq. (3) is then used to obtain average calculated and measured mass scattering efficiency at each site.

$$\alpha_{sp,avg,i} = \frac{b_{sp,avg,i}}{PM_{10,avg,i}} \quad (3)$$

Although the OPTEC open air nephelometer reduces truncation error compared with other nephelometers, truncation error can be significant for coarse particles (Hand and Malm, 2007; Lowenthal and Kumar, 2006). Thus our analysis below focuses on conditions dominated by fine mode aerosols, and mechanisms affecting fine mode aerosols.

Appendix A describes the calculation of mass scattering efficiency in more detail. This approach enables isolation of the mass scattering efficiencies used in GEOS-Chem from the species concentrations.

2.4 Introducing an alternate hygroscopic growth scheme

We examine for GEOS-Chem the use of a widely adopted alternate hygroscopic growth scheme, in which aerosol hygroscopic growth is defined by a single parameter, κ (Petters and Kreidenweis 2007, 2008, 2013). This representation of water uptake by aerosols was originally developed for supersaturated CCN conditions, but in recent years has been used extensively in subsaturated conditions (Dusek et al., 2011; Hersey et al., 2013).

Deleted:

Formatted: Justified

Deleted:

Deleted: at

Deleted: 3

The hygroscopic parameter κ is defined by

$$\frac{1}{a_w} = 1 + \kappa \frac{V_d}{V_w} \qquad (4)$$

Deleted: 3

where V_d is dry particulate matter volume, V_w is the water volume and a_w is water activity (Petters and Kreidenweis, 2013), which is unity for secondary inorganic aerosols (SIA) and organic aerosols (OA). The diameter growth factor ($GF=D/D_d$) can be expressed (Snider et al., 2016) as

$$GF = \left(1 + \kappa \frac{RH}{100-RH}\right)^{1/3} \qquad (5)$$

Deleted: κ_v

Deleted: 4

where D is the wet aerosol radius and D_d is the dry aerosol radius. Typically, κ is in the range of 0.5-0.7 for SIA (Hersey et al., 2013; Kreidenweis et al., 2008; Petters & Kreidenweis, 2007) and 0-0.2 for OA (Duplissy et al., 2011; Kreidenweis et al., 2008; Rickards et al., 2013; Snider et al., 2016).

Deleted: $_v$

3. Results

3.1 Understanding the current representation of α_{sp}

Figure 2 (left) shows measured vs. calculated mass scattering efficiency using GEOS-Chem default optical tables. Each point represents the average α_{sp} over the entire sampling period at each IMPROVE site. A significant correlation (r=0.94) is apparent, however a bias in α_{sp} is evident. A positive correlation between average mass scattering efficiency and RH is apparent; sites with low average RH have low average α_{sp} and vice versa. (The right panel of Figure 2 is discussed below.)

Deleted: at an

Deleted: over the entire sampling period

Deleted: 6

To further investigate the RH dependence of this bias, we separate our analysis of calculated α_{sp} into 3 relative humidity groupings: 0-35% (low), 35-65% (mid) and 65-95% (high). The IMPROVE data is divided among the RH groupings using IMPROVE measurements of hourly RH. Within each grouping, average calculated and measured mass scattering efficiencies are obtained for each site using Eq. (3). The blue dots in Fig. 3 show average calculated vs measured α_{sp} for each RH range. In the low RH case, a significant overestimation of mass scattering efficiency is apparent at most sites, with a bias of 82% indicated by the slope. In the mid RH case, overestimation of α_{sp} is less significant but still apparent with a bias of 40% indicated by the slope. At high RH, bias is weak.

Formatted: Font color: Auto

Formatted: Font color: Auto

Formatted: Font color: Auto

Deleted: 7

Deleted: 38

To further understand the source of the bias in calculated mass scattering efficiency, we now examine calculated α_{sp} in conditions dominated by different aerosol types. Using IMPROVE measurements of 24 hr $PM_{2.5}$ mass and speciation and PM_{10} mass, the IMPROVE data is grouped based on dominant aerosol type. Within each group, average calculated and measured mass scattering efficiency is obtained for each site using Eq. (3). Figure 4 shows in blue average measured vs calculated α_{sp} using default optical tables for conditions where measured $PM_{2.5}$ is dominated (>60%) by secondary inorganic aerosol, organic aerosol and fine dust, as well conditions where PM_{10} is dominated (>60%) by PM_{coarse} (PM_{10}-$PM_{2.5}$). The scatterplot in the SIA dominant case resembles the overall relationship shown in Fig. 2. α_{sp} is overestimated at most sites, with significant correlation (r=0.88), and a bias evident in the offset of 0.70. Where OA is the dominant component of $PM_{2.5}$,

Deleted: 9

Deleted: 2

the slope is close to unity (1.02) but the large offset of 0.80 $m^2 g^{-1}$ results in α_{sp} being largely overestimated. Where dust is the dominant fine aerosol, correlation is significant (r=0.89) and mass scattering efficiency is accurately calculated at the vast majority of sites, despite a prominent outlier at a site in the Columbia River Gorge, Washington. The PM_{coarse} dominant case shows significant correlation (r=0.88) and a slight tendency for overestimation of α_{sp}. As this case is not independent from the other cases, this overestimation is likely linked to the overestimation in the OA and SIA dominant cases as demonstrated below.

These results indicate that the bias in calculated mass scattering efficiency arises mostly due to the representation of the physical and optical properties of secondary inorganic and organic aerosols. The following will focus on improving the representation of physical and optical properties of these two aerosol types.

3.2 Changing the physical properties of SIA and OA

Figure 5 shows mass scattering efficiency as a function of aerosol size for secondary inorganic (orange) and organic (blue) aerosols for dry aerosols (solid) and aerosols at 80% RH (dashed lines) as calculated using a Mie algorithm ((Mishchenko et al., 1999). Water uptake at 80% RH for OA and SIA is calculated using default hygroscopic growth factors from GEOS-Chem. The uptake of water increases aerosol scatter, decreases aerosol density and decreases the refractive index. The increase in aerosol scatter with increasing ambient RH drives the increase in α_{sp}.

The points in Fig. 5 represent the current mass scattering efficiency values of OA and SIA in GEOS-Chem. For dry aerosols, α_{sp}=4.4 $m^2 g^{-1}$ for OA and α_{sp}=3.2 $m^2 g^{-1}$ for SIA. In a review of ground-based estimates of aerosol mass scattering efficiencies, Hand et al. (2007) found dry α_{sp} values of 2.5 $m^2 g^{-1}$ for ammonium sulfate, 2.7 $m^2 g^{-1}$ for ammonium nitrate, and 3.9 $m^2 g^{-1}$ for particulate organic matter. These values suggest that the default optical tables in GEOS-Chem currently overestimate mass scattering efficiency of SIA and OA in dry conditions. This reaffirms the overestimation of α_{sp} in dry conditions evident in the left panel of Fig. 3. As aerosol size is the strongest determinant of dry mass scattering efficiency, we begin by examining the dry sizes of SIA and OA in GEOS-Chem.

The current dry sizes of SIA and OA in GEOS-Chem were informed by measurements from several aircraft campaigns over eastern North America during the summer of 2004 (Drury et al., 2010) as part of the The International Consortium for Atmospheric Research on Transport and Transformation (ICARTT) (Fehsenfeld et al., 2006; Singh et al., 2006). Aerosol surface area and volume distributions fluctuate seasonally in the North Eastern U.S., with summer maxima and winter minima (Stanier et al., 2004). We divide our analysis at low RH by season, in an effort to discern a seasonal pattern in the overestimation of α_{sp}.

Figure 6 (blue) shows seasonal measured vs. calculated mass scattering efficiency in dry conditions using default optical tables (Table A1). Estimations of α_{sp} are most accurate in the summer, consistent with the dry sizes chosen by Drury et al. (2010) which were informed by summertime size distribution measurements. The larger overestimation of α_{sp} in all

Deleted: 0.99

Deleted: 7

Deleted: 90

other seasons, most notably in winter, is consistent with the seasonality in aerosol size distributions observed by Stanier et al. (2004).

3.2.1 Efflorescence relative humidity

To address the overestimation of mass scattering efficiency in dry conditions illustrated in Fig. 3 and Fig. 6, we begin by accounting for efflorescence transitions in secondary inorganic aerosols. Efflorescence phase transitions are characterized by nucleation of the crystalline phase followed by rapid evaporation of water. Field measurements have found evidence for these transitions (Martin et al., 2008). The efflorescence relative humidity (ERH) of ammonium sulfate reported in several experimental studies range from 35-40% (Ciobanu et al., 2010). Laboratory tests have shown that mixtures of sulfate-nitrate-ammonium particles will undergo efflorescence when the ammonium sulfate fraction is high (Dougle et al., 1998; Martin et al., 2003). This condition is true at most global measurement sites, with the possible exception of Europe, where particles are nitrate rich (Martin et al., 2003).

We therefore define the hygroscopic growth factor for SIA as unity for RH ≤ 35%, linearly increasing between 35-40% RH from unity to GF$_{40\%}$ (calculated by Eq. (5)), and following the default (or κ-Kohler) growth curve for RH ≥ 40%. Incorporating an ERH for SIA and consequently inhibiting hygroscopic growth of SIA below 35% RH significantly reduces the overestimation of mass scattering efficiency in dry conditions. In the case of default hygroscopic growth in GEOS-Chem, the overall dry bias in α_{sp} is reduced from 82% to 48%.

Deleted: 4

Formatted: Not Highlight

Deleted: 7

Formatted: Not Highlight

Deleted: 53

3.2.2 Aerosol dry size

To address the remaining overestimation of mass scattering efficiency in dry conditions we explore different dry sizes of secondary inorganic and organic aerosols. Effective variance may also be important (Chin et al., 2002) but given insufficient information to simultaneously constrain size and variance, we focus on size. Figure 7 shows the slope of the average measured vs calculated α_{sp} plot for RH<35% for dry radii ranging from 0.048 to 0.074 μm at intervals of 0.001 μm, assuming SIA and OA have the same dry size. The slope of the best fit line acts as an indicator of the appropriate dry size for each season. Sensitivity tests exploring alternative error metrics (RMSE, MSE) yielded similar results. The slope decreases steadily as dry radius is decreased in all seasons. Using the dry radius which gives a slope of unity, we find that aerosols are largest in summer (r=0.067 μm), smallest in winter (r=0.051 μm), and in between in spring and fall (0.059 μm and 0.054 μm, respectively). The spring and summer radii are consistent with accumulation mode size distribution measurements performed by Levin et al. (2009) in the spring and summer of 2006. Averaging the sizes from all four seasons results in an annual representative dry radius of 0.058 μm. This annual radius is smaller than the GEOS-Chem default sizes of SIA and OA that were informed by summertime measurements alone (Drury et al., 2010).

Deleted: 50

Deleted: Slope as a function of radius is nearly identical in the spring and fall, diverging slightly for the smallest sizes.

Deleted: 2

Deleted: 7

Deleted: 6

Deleted: (

Deleted: ,

Figure 6 (red) shows seasonal measured vs. calculated α_{sp} in dry conditions using new representative annual geometric mean radius of 0.058 μm for SIA and OA. This change in geometric mean radius reduces the overestimation of

Deleted: this

α_{sp} in all seasons, with the largest improvement in fall (slope decreases from 1.84 to 1.17) and winter (slope decreases from 1.94 to 1.20). Changes in correlation are minor. For the remainder of the analysis, this new dry radius of 0.058 μm is implemented for SIA and OA.

3.2.3 Aerosol hygroscopicity

We now examine the implementation of the widely adopted κ-Kohler hygroscopic growth scheme described in section 2.4. A range of measured κ values for SIA (κ_s) and OA (κ_o) exist in the literature. We explore the range of possible κ values, using the slope of the measured vs calculated α_{sp} plot as an indicator of the appropriate values.

Figure 8 shows the slope of the measured vs calculated α_{sp} plot for κ values for SIA (κ_s) ranging from 0.5-0.7 and for OA (κ_o) ranging from 0.08-0.20. Slope increases steadily as κ_s and κ_o increase. A slope of unity identifies representative values of κ_s=0.61 and κ_o=0.10. These values are in the middle of the range of measured κ values (Duplissy et al., 2011; Hersey et al., 2013; Kreidenweis et al., 2008; Petters and Kreidenweis, 2007; Rickards et al., 2013).

Figure 9 shows the diameter growth factor as a function of relative humidity following κ-Kohler theory, as well as GADS hygroscopic growth for both SIA and OA used in the default GEOS-Chem model. Hygroscopic growth from the Aerosol Inorganic Model (AIM) at T=298 K (Wexler and Clegg, 2002) and laboratory measurements (Wise et al., 2003) are also shown for ammonium sulfate (Snider et al., 2016). The GADS hygroscopic growth schemes used in the default GEOS-Chem simulation are characterized by larger growth at low RH and smaller growth at high RH for both secondary inorganic and organic aerosols. The κ-Kohler scheme exhibits greater consistency with both AIM and laboratory hygroscopic growth for SIA.

Using the revised dry size of 0.058 μm and the κ-Kohler theory of hygroscopic growth, we calculate revised physical and optical properties for SIA and OA over a range of RH values. Table A1 contains geometric mean radius, extinction efficiency and single scattering albedo for the revised optical tables at 8 relative humidity values.

Figure 2 (right) shows the measured vs calculated mass scattering efficiency using these revised optical tables for SIA and OA. The overestimation of mass scattering efficiency has been eliminated with these revised aerosol properties, with a slope of 1.00 and an offset of 0.09. Correlation remains significant at r=0.96.

Figure 4 (red) shows measured vs calculated α_{sp} in conditions dominated by different aerosol types using the revised optical tables. The overestimation of α_{sp} in SIA dominant conditions using the default optical tables has been eliminated, with a slope of 1.03 and a decreased offset (0.70 to 0.1). The large overestimation of α_{sp} that was apparent in OA dominant conditions has been reduced by a factor of 2. α_{sp} remains accurately estimated at the majority of dust dominant sites, with the outlier at the Columbia River Gorge site in Washington still skewing the best fit line. The slight overestimation of α_{sp} that was present in the PM_{coarse} dominant case using default optical tables has been eliminated using the revised tables (offset 0.33 to 0.03). Slight increases in correlation coefficients are apparent in all cases except for the SIA dominant case, where it decreased by 0.02.

Deleted: spring

Deleted: 73

Deleted: 01

Deleted: .8

Deleted: 7

Deleted: 16

Deleted:

Deleted: 3

Deleted: 58

Deleted: 5

Deleted: 7

Deleted: 0

Deleted: 9

Deleted: 6

Deleted: Moderate

Figure 3 (red) shows measured vs calculated α_{sp} using revised optical tables. The overestimation in α_{sp} has been significantly reduced in the low RH case (slope=1.82 to slope=1.09) and in the mid RH case (slope=1.40 to slope=1.01) compared to when default optical tables were used. The slight overestimation in high RH conditions present in the default case has also been reduced, as shown by the decreased offset (0.90 to 0.71).

Deleted: 7
Deleted: 13
Deleted: 38
Deleted: 0.98
Deleted: 84
Deleted: 65
Deleted:

3.3 Changes in GEOS-Chem simulated α_{sp}

Here, we examine how these changes to aerosol properties impact both GEOS-Chem simulation of mass scattering efficiency over North America and the fit between modeled and measured α_{sp} at IMPROVE sites. These simulations rely on GEOS-Chem simulations of aerosol composition using GEOS RH fields.

Figure 10 shows the relative and absolute change in mass scattering efficiency when switching from the default to revised optical tables. Continental mean α_{sp} increased by 16%. Increases in α_{sp} range from 25-45% in northeastern regions of North America, corresponding to an increase of 1.5-3.5 m^2 g^{-1}. These larger changes reflect the higher RH and SIA fractions. Decreases in α_{sp} of up to 15% or -0.5 m^2 g^{-1} are found in the southwest where RH is low and mineral dust dominates.

Deleted: 2
Deleted: 0
Deleted: 0
Formatted: Not Highlight

Figure 11 shows GEOS-Chem annual average mass scattering efficiency using default (top) and revised (bottom) optical tables over North America for the year 2006. The overlaying circles represent average measured α_{sp} at IMPROVE network sites for the year 2006, and the outer rings show the coincident simulated α_{sp} for each site. We exclude sites within 1° of the coast where sea-salt affects α_{sp}, as well as sites where elevation differs from average gridbox elevation by more than 1500 meters. These criteria result in a decrease from 24 to 19 in the number of sites available for the analysis in 2006.

Using default optical tables, simulated continental mean α_{sp} is 5.4 m^2 g^{-1}. A maximum α_{sp} of 10 m^2 g^{-1} occurs in British Columbia, and a minimum α_{sp} of 1.7 m^2 g^{-1} occurs in the southwest United States. Using revised optical tables, simulated continental mean α_{sp} is 6.3 m^2 g^{-1}, with a maximum of 12.5 m^2 g^{-1} in the northwest, and a minimum of 1.5 m^2 g^{-1} in the southwest. The elevated mass scattering efficiencies in the northwest can be attributed in part to the high average RH in this region of 83%.

Deleted: 2
Deleted: 2

Figure 12 (left) shows coincident measured vs simulated mass scattering efficiency at the 19 IMPROVE sites, using default optical tables. Correlation is significant (r=0.88), but a bias in simulated α_{sp} is apparent (slope=0.83). Simulated α_{sp} is notably biased low at sites in the southeastern United States where average α_{sp} is largest, and simulated α_{sp} is notably biased high at sites in the southwestern United States where average mass scattering efficiency is lowest. Sites with lowest average RH correspond to those with the lowest average mass scattering efficiency and vice versa. The tendency of mass scattering efficiency to be overestimated at low RH reflects the tendency that was originally seen in Fig. 4.

Figure 12 (right) shows coincident measured vs simulated α_{sp} using revised optical tables. Correlation remains significant (r=0.89), and a decrease in bias is evident from the increase in slope (0.83 to 0.93) and decrease in offset (0.47 to

Deleted: 0

0.08). Most sites now lie closer to the 1:1 line. The overestimation of simulated α_{sp} in the southwest, where RH is low, has been reduced or eliminated at all sites.

Deleted: 10

3.4 Comparison with AERONET measurements

Appendix B investigates changes to simulated AOD, and compares measured and simulated AOD at AERONET sites. Although large relative increases upwards of 60% in average AOD are evident in large parts of northern high-latitudes where absolute AOD is small, absolute AOD generally changes by less than 0.1 (Fig. B1). Comparisons with AERONET AOD reveal that the revised optical properties slightly improve the simulation of AOD worldwide (slope decreases from 1.08 to 1.00) despite the large influence of other factors (e.g. ambient aerosol concentrations) upon AOD.

Deleted: 0.99

4. Conclusions

The current representation of mass scattering efficiency in the GEOS-Chem global chemical transport model was evaluated using collocated ground-based measurements of particle mass, speciation, scatter and relative humidity from the IMPROVE network.

Calculated mass scattering efficiency had a positive bias using default physical and optical properties used in the GEOS-Chem model. This bias was most significant when $PM_{2.5}$ mass was dominated by secondary inorganic (SIA) or organic aerosols (OA). Mass scattering efficiency in $PM_{2.5}$ dust and coarse particulate matter dominant conditions was accurately represented at the majority of IMPROVE sites.

Deleted: ere

Relative humidity played an important role in the severity of the bias in mass scattering efficiency. Mean α_{sp} was overestimated by 82% in dry conditions (RH<35%). This bias was largest in the winter (94%) and smallest in the summer (27%). Implementing an efflorescence relative humidity for SIA and thus inhibiting hygroscopic growth below 35% RH decreased the dry bias by 34%. An annual representative dry geometric mean radius of 0.058 µm for SIA and OA decreased the dry mass scattering efficiency of these aerosols, and subsequently further reduced the bias in dry conditions to 9%.

Deleted: 7

Deleted: 87

Deleted: 9

Deleted: 13

κ-Kohler theory was implemented for the hygroscopic growth of SIA and OA, which is characterized by smaller growth factors at low RH and larger growth factors at high RH compared to default growth factors in GEOS-Chem. κ values of 0.61 for SIA and 0.10 for OA eliminated the overall bias in calculated mass scattering efficiency.

Deleted: 58

These changes to SIA and OA optical tables resulted in a continental mean increase in GEOS-Chem simulated mass scattering efficiency of 16%. Northeastern regions of North America exhibited the largest increases (25-45%) due to high RH and SIA fractions, while southwestern regions of the continent exhibited decreases in α_{sp} of up to 15% due to low RH and high dust fractions. These changes to the GEOS-Chem optical tables improved the fit between measured and simulated mass scattering efficiency at IMPROVE sites, reflected in the changes to the slope (0.83 to 0.93) and the offset (0.47 to 0.08).

Deleted: 2

Deleted: 0

Deleted: 0

Deleted: 0

Deleted: 10

Future work should examine the implications of these changes for satellite-derived estimates of fine particulate matter that depend on the relationship of AOD with $PM_{2.5}$. Future work should also expand analysis of the representation of mass scattering efficiency for other years, and by incorporating measurements from other ground based measurement networks such as the Surface PARTiculate MAtter network (SPARTAN), which provides measurements of particulate mass, speciation and scatter in populated regions worldwide (Snider et al., 2015; Snider et al., 2016). Such comparisons may also be useful to evaluate and improve prognostic simulations of aerosol size (Mann et al., 2010; Spracklen et al., 2005; Trivitayanurak et al., 2008; Yu and Luo, 2009) . Representation of particle RH history may also be important (Wang et al., 2008).

Appendix A

A.1 b_{sp} and α_{sp} calculations in GEOS-Chem

In GEOS-Chem, surface level b_{sp} is calculated using model particle mass concentrations and local relative humidity, as well as predefined mass densities and aerosol optical properties for each aerosol component following:

$$b_{sp} = \sum_{species,i} \frac{\frac{3}{4} * \left(\frac{R_{w,i}}{R_{d,i}}\right)^2 * M_{d,i} * Q_{w,i} * SSA_{w,i}}{\rho_{d,i} * R_{d,i}} \qquad \text{(A1)}$$

where ρ_d is the dry particle mass density, R_w is the effective radius (defined as the ratio of the third to second moment of an aerosol size distribution), R_d is the dry effective radius, M_d is the dry surface level mass concentration, Q_w is the extinction efficiency, and SSA_w is the single scattering albedo. Parameters with the subscript w indicate values at ambient RH. Species included in this calculation are SO_4^{2-}, NH_4^+, NO_3^-, BC, OM and fine and coarse dust and sea salt.

Dividing Eq. (A1) by total surface level PM_{10} results in the following equation for mass scattering efficiency

$$\alpha_{sp} = \frac{B_{sp}}{PM_{10}} = \frac{\sum_{species,i} \frac{\frac{3}{4} * \left(\frac{R_{w,i}}{R_{d,i}}\right)^2 * \frac{M_{d,i}}{PM_{10}} * Q_{w,i} * SSA_{w,i}}{\rho_{d,i} * R_{d,i}}}{PM_{10}} \qquad \text{(A2)}$$

The effective radius, extinction efficiency and single scattering albedo in Eq. (A1) and (A2) are obtained from GEOS-Chem optical tables for the ambient RH values measured by IMPROVE. Dry mass density ρ_d is specified for each aerosol species in GEOS-Chem (Table A2). $M_{d,i}$ and PM_{10} are obtained from IMPROVE network measurements of aerosol mass and composition. α_{sp} calculated by Eq. (A2) is compared to α_{sp} directly measured by the IMPROVE network.

Mass scattering efficiency is dependent on particle density, refractive index and particle size. Mass scattering efficiency is typically most dependent on aerosol size, which is dictated by both the dry size distribution chosen to represent a given aerosol species, and by the hygroscopic growth scheme used to represent aerosol water uptake for hydrophilic species.

Deleted: 5

Deleted: $\sum_{species,i} \frac{\frac{3}{4} * \left(\frac{R_{w,i}}{R_{d,i}}\right)^2 * \frac{M_{d,i}}{PM_{10}} * Q_{w,i} * SSA_{w,i}}{\rho_{d,i} * R_{d,i}}$

A.2 Incorporating IMPROVE Network Measurements

The IMPROVE network measures every three days $PM_{2.5}$ mass and speciation and PM_{10} mass. The IMPROVE particle sampler consists of four independent modules with separate inlets and pumps. The first three modules (A, B and C) collect only fine particulate matter ($PM_{2.5}$), while the 4th module (D) collects both fine and coarse particles (PM_{10}). Module A collects $PM_{2.5}$ on a Teflon filter, which undergoes gravimetric analysis for total $PM_{2.5}$ mass and x-ray florescence for elemental concentrations (including Al, Si, Ca, Fe, Ti). The nylon filter in module B undergoes ion chromatography analysis for SO_4^{2-}, NO_3^-, NO_2^- and Cl^-. Module C contains a quartz filter that is analyzed for organic and elemental carbon via thermal optical reflectance. The Teflon filter in module D undergoes gravimetric analysis for PM_{10} mass (Malm et al., 1994; Malm et al., 2004). Prior to gravimetric analysis, filters A and D undergo equilibration at 30-50% RH and 20-25 °C for several minutes (Solomon et al., 2014).

The GEOS-Chem model partitions OM into hydrophilic and hydrophobic fractions, so the same is done for OM measured by IMPROVE to enable isolation of mass scattering efficiency in our comparisons. OM in remote regions tends to be highly oxidized, and oxidation level of organics has been shown to positively correlate with hygroscopicity (Duplissy et al., 2011; Jimenez et al., 2009; Ng et al., 2010). We treat measured OM as 90% hydrophilic, due to the rural nature of IMPROVE sites. EC is treated as 50% hydrophilic. As speciation of coarse material is unavailable, we treat all coarse material as crustal in origin, an assumption that may breakdown at coastal sites. We partition fine and coarse dust measured by the IMPROVE network into the GEOS-Chem size bins using the dust particle size distribution (PSD) described by Zhang et al. (2013).

Appendix B

The *Ae*rosol *Ro*botics *Net*work (AERONET) is a long-term network of ground based sun photometers that provides continuous, cloud-screened measurements of aerosol optical depth (AOD) at several fixed wavelengths in the visible and near infrared (Holben et al., 1998). The calculation of AOD in GEOS-Chem is performed using simulated mass concentrations of aerosol species and mass extinction efficiencies, summed over all vertical layers. Our analysis of mass scattering efficiency can therefore be extended globally by comparing GEOS-Chem calculated AOD to AOD measured at AERONET sites. During our simulation year of 2006, AERONET consisted of 231 sites across the globe.

Here we examine how the changes to SIA and OA properties impact GEOS-Chem simulated AOD globally. Figure B1 shows the relative (top) and absolute (bottom) changes in AOD. Global mean AOD increases by 19%. Relative changes in AOD are most pronounced in Northern regions where mean relative humidity is high, with increases in simulated AOD ranging from 50-90%. Decreases in AOD between 0-20% are present in most of the southern hemisphere, in part due to the lower average RH. Absolute changes in AOD show a similar tendency, with slight increases in AOD of up to 0.2 in northern regions, and slight decreases of up of -0.09 in southern regions. An exception to this is seen over parts of China, where AOD increases by 0.5 due to the elevated SIA and OA concentrations.

Formatted: Not Highlight

Deleted: 8

Figure B2 shows coincident measured (inner circles) and simulated (outer rings) AOD for the year 2006 using default optical tables (top) and revised optical tables (bottom). We exclude sites within 1° of the coast, as well as sites where elevation differs from average gridbox elevation by more than 1500 meters. We also exclude sites where average $PM_{2.5}$ is dominated by dust (dust/$PM_{2.5}$>0.6), to focus on the representation of the optical properties of SIA and OA. Across the globe, we see that AOD is both over and underestimated. AOD is overestimated at most sites in Africa, with the most notable overestimation at the site in Nigeria. AOD is moderately overestimated at sites in Australia. Underestimation of AOD occurs at most sites in South America, as well as at sites in southern North America and southern Asia.

Figure B3 shows coincident measured vs simulated AOD at AERONET sites for default (left) and revised (right) optical tables. The correlation coefficient (r=0.80 to r=0.78) changes insignificantly, while the slope decreases from 1.08 to 1.00 when switching to the revised optical tables. In summary, the revised optical properties developed for North America slightly improve the representation of AOD at the global scale, despite the large influence of other factors (e.g. ambient aerosol concentrations and composition) upon AOD.

Deleted: 0.99

Data Availability

IMPROVE network data for 2000-2010 can be accessed at http://vista.cira.colostate.edu/Improve/improve-data/.

Deleted: 5

Acknowledgements

Research described in this article was conducted under contract to the Health Effects Institute (HEI), an organization jointly funded by the United States Environmental Protection Agency (EPA) (Assistance Award No. R-82811201) and certain motor vehicle and engine manufacturers. The contents of this article do not necessarily reflect the views of HEI, or its sponsors, nor do they necessarily reflect the views and policies of the EPA or motor vehicle and engine manufacturers.

IMPROVE is a collaborative association of state, tribal, and federal agencies, and international partners. US Environmental Protection Agency is the primary funding source, with contracting and research support from the National Park Service. The Air Quality Group at the University of California, Davis is the central analytical laboratory, with ion analysis provided by Research Triangle Institute, and carbon analysis provided by Desert Research Institute.

We thank Environment and Climate Change Canada for providing nephelometer data at the site in Egbert, Ontario.

Deleted:

Formatted: Normal

References

Achakulwisut, P., Shen, L. and Mickley, L. J.: What Controls Springtime Fine Dust Variability in the Western United

States? Investigating the 2002–2015 Increase in Fine Dust in the U.S. Southwest, J. Geophys. Res. Atmos., 122(22), 12,412-449,467, doi:10.1002/2017JD027208, 2017.

Andrews, E., Ogren, J. A., Bonasoni, P., Marinoni, A., Cuevas, E., Rodríguez, S., Sun, J. Y., Jaffe, D. A., Fischer, E. V., Baltensperger, U., Weingartner, E., Coen, M. C., Sharma, S., Macdonald, A. M., Leaitch, W. R., Lin, N. H., Laj, P., Arsov, T., Kalapov, I., Jefferson, A. and Sheridan, P.: Climatology of aerosol radiative properties in the free troposphere, Atmos. Res., 102(4), 365–393, doi:10.1016/j.atmosres.2011.08.017, 2011.

Bey, I., Jacob, D. J., Yantosca, R. M., Logan, J. A., Field, B. D., Fiore, A. M., Li, Q.-B., Liu, H.-Y., Mickley, L. J. and Schultz, M. G.: Global Modeling of Tropospheric Chemistry with Assimilated Meteorology: Model Description and Evaluation, J. Geophys. Res., 106, 73–95, doi:10.1029/2001JD000807, 2001.

Chin, M., Ginoux, P., Kinne, S., Torres, O., Holben, B. N., Duncan, B. N., Martin, R. V., Logan, J. a., Higurashi, A. and Nakajima, T.: Tropospheric Aerosol Optical Thickness from the GOCART Model and Comparisons with Satellite and Sun Photometer Measurements, J. Atmos. Sci., 59(3), 461–483, doi:10.1175/1520-0469(2002)059<0461:TAOTFT>2.0.CO;2, 2002.

Ciobanu, V. G., Marcolli, C., Krieger, U. K., Zuend, A. and Peter, T.: Efflorescence of ammonium sulfate and coated ammonium sulfate particles: Evidence for surface nucleation, J. Phys. Chem. A, 114(35), 9486–9495, doi:10.1021/jp103541w, 2010.

Collaud Coen, M., Andrews, E., Asmi, A., Baltensperger, U., Bukowiecki, N., Day, D., Fiebig, M., Fjaeraa, A. M., Flentje, H., Hyvärinen, A., Jefferson, A., Jennings, S. G., Kouvarakis, G., Lihavainen, H., Lund Myhre, C., Malm, W. C., Mihapopoulos, N., Molenar, J. V., O'Dowd, C., Ogren, J. A., Schichtel, B. A., Sheridan, P., Virkkula, A., Weingartner, E., Weller, R. and Laj, P.: Aerosol decadal trends-Part 1: In-situ optical measurements at GAW and IMPROVE stations, Atmos. Chem. Phys., 13(2), 869–894, doi:10.5194/acp-13-869-2013, 2013.

van Donkelaar, A., Martin, R. V., Brauer, M., Kahn, R., Levy, R., Verduzco, C. and Villeneuve, P. J.: Global estimates of ambient fine particulate matter concentrations from satellite-based aerosol optical depth: Development and application, Environ. Health Perspect., 118(6), 847–855, doi:10.1289/ehp.0901623, 2010.

van Donkelaar, A., Martin, R. V, Spurr, R. J. D. and Burnett, R. T.: High-Resolution Satellite-Derived PM2.5 from Optimal Estimation and Geographically Weighted Regression over North America, Environ. Sci. Technol., 49(17), 10482–10491, doi:10.1021/acs.est.5b02076, 2015.

Dougle, P. G., Veefkind, J. P. and R, H. M. B.: Crystallisation of mixtures of ammonium nitrate, ammonium sulphate and soot, , 29(3), 375–386, 1998.

Drury, E., Jacob, D. J., Spurr, R. J. D., Wang, J., Shinozuka, Y., Anderson, B. E., Clarke, A. D., Dibb, J., McNaughton, C. and Weber, R.: Synthesis of satellite (MODIS), aircraft (ICARTT), and surface (IMPROVE, EPA-AQS, AERONET) aerosol observations over eastern North America to improve MODIS aerosol retrievals and constrain surface aerosol concentrations and sources, J. Geophys. Res. Atmos., 115(14), 1–17, doi:10.1029/2009JD012629, 2010.

Duplissy, J., De Carlo, P. F., Dommen, J., Alfarra, M. R., Metzger, A., Barmpadimos, I., Prevot, A. S. H., Weingartner, E., Tritscher, T., Gysel, M., Aiken, A. C., Jimenez, J. L., Canagaratna, M. R., Worsnop, D. R., Collins, D. R., Tomlinson, J. and Baltensperger, U.: Relating hygroscopicity and composition of organic aerosol particulate matter, Atmos. Chem. Phys., 11(3), 1155–1165, doi:10.5194/acp-11-1155-2011, 2011.

Dusek, U., Frank, G. P., Massling, A., Zeromskiene, K., Iinuma, Y., Schmid, O., Helas, G., Hennig, T., Wiedensohler, A. and Andreae, M. O.: Water uptake by biomass burning aerosol at sub-and supersaturated conditions: Closure studies and implications for the role of organics, Atmos. Chem. Phys., 11(18), 9519–9532, doi:10.5194/acp-11-9519-2011, 2011.

Fairlie, D. T., Jacob, D. J. and Park, R. J.: The impact of transpacific transport of mineral dust in the United States, Atmos. Environ., 41(6), 1251–1266, doi:10.1016/j.atmosenv.2006.09.048, 2007.

Fairlie, T. D., Jacob, D. J., Dibb, J. E., Alexander, B., Avery, M. A., Van Donkelaar, A. and Zhang, L.: Impact of mineral dust on nitrate, sulfate, and ozone in transpacific Asian pollution plumes, Atmos. Chem. Phys., 10(8), 3999–4012, doi:10.5194/acp-10-3999-2010, 2010.

Fehsenfeld, F. C., Ancellet, G., Bates, T. S., Goldstein, A. H., Hardesty, R. M., Honrath, R., Law, K. S., Lewis, A. C., Leaitch, R., McKeen, S., Meagher, J., Parrish, D. D., Pszenny, A. A. P., Russell, P. B., Schlager, H., Seinfeld, J., Talbot, R. and Zbinden, R.: International Consortium for Atmospheric Research on Transport and Transformation (ICARTT): North America to Europe - Overview of the 2004 summer field study, J. Geophys. Res. Atmos., 111(23), doi:10.1029/2006JD007829, 2006.

Fountoukis, C. and Nenes, A.: ISORROPIA II: a computationally efficient thermodynamic equilibrium model for K –H 2 O aerosols, Atmos. Chem. Phys. Atmos. Chem. Phys., 7, 4639–4659, doi:10.5194/acp-7-4639-2007, 2007.

Gebhart, K. A., Copeland, S. and Malm, W. C.: Diurnal and seasonal patterns in light scattering, extinction, and relative humidity, Atmos. Environ., 35(30), 5177–5191, doi:10.1016/S1352-2310(01)00319-3, 2001.

Gelaro, R., McCarty, W., Suárez, M. J., Todling, R., Molod, A., Takacs, L., Randles, C. A., Darmenov, A., Bosilovich, M. G., Reichle, R., Wargan, K., Coy, L., Cullather, R., Draper, C., Akella, S., Buchard, V., Conaty, A., da Silva, A. M., Gu, W., Kim, G. K., Koster, R., Lucchesi, R., Merkova, D., Nielsen, J. E., Partyka, G., Pawson, S., Putman, W., Rienecker, M., Schubert, S. D., Sienkiewicz, M. and Zhao, B.: The modern-era retrospective analysis for research and applications, version 2 (MERRA-2), J. Clim., 30(14), 5419–5454, doi:10.1175/JCLI-D-16-0758.1, 2017.

Hand, J. L. and Malm, W. C.: Review of aerosol mass scattering efficiencies from ground-based measurements since 1990, J. Geophys. Res. Atmos., 112(16), doi:10.1029/2007JD008484, 2007.

Hersey, S. P., Craven, J. S., Metcalf, A. R., Lin, J., Lathem, T., Suski, K. J., Cahill, J. F., Duong, H. T., Sorooshian, A., Jonsson, H. H., Shiraiwa, M., Zuend, A., Nenes, A., Prather, K. A., Flagan, R. C. and Seinfeld, J. H.: Composition and hygroscopicity of the Los Angeles Aerosol: CalNex, J. Geophys. Res. Atmos., 118(7), 3016–3036, doi:10.1002/jgrd.50307, 2013.

Holben, B. N., Eck, T. F., Slutsker, I., Tanré, D., Buis, J. P., Setzer, A., Vermote, E., Reagan, J. A., Kaufman, Y. J., Nakajima, T., Lavenu, F., Jankowiak, I. and Smirnov, A.: AERONET—A Federated Instrument Network and Data Archive for Aerosol Characterization, Remote Sens. Environ., 66(1), 1–16, doi:10.1016/S0034-4257(98)00031-5, 1998.

Hyslop, N. P. and White, W. H.: An evaluation of interagency monitoring of protected visual environments (IMPROVE) collocated precision and uncertainty estimates, Atmos. Environ., 42(11), 2691–2705, doi:10.1016/j.atmosenv.2007.06.053, 2008.

Jaeglé, L., Quinn, P. K., Bates, T. S., Alexander, B. and Lin, J. T.: Global distribution of sea salt aerosols: New constraints from in situ and remote sensing observations, Atmos. Chem. Phys., 11(7), 3137–3157, doi:10.5194/acp-11-3137-2011, 2011.

Jimenez, J. L., Canagaratna, M. R., Donahue, N. M., Prevot, a. S. H., Zhang, Q., Kroll, J. H., DeCarlo, P. F., Allan, J. D., Coe, H., Ng, N. L., Aiken, a. C., Docherty, K. S., Ulbrich, I. M., Grieshop, A. P., Robinson, a. L., Duplissy, J., Smith, J. D., Wilson, K. R., Lanz, V. a., Hueglin, C., Sun, Y. L., Tian, J., Laaksonen, A., Raatikainen, T., Rautiainen, J., Vaattovaara, P., Ehn, M., Kulmala, M., Tomlinson, J. M., Collins, D. R., Cubison, M. J., Dunlea, J., Huffman, J. A., Onasch, T. B., Alfarra, M. R., Williams, P. I., Bower, K., Kondo, Y., Schneider, J., Drewnick, F., Borrmann, S., Weimer, S., Demerjian, K., Salcedo, D., Cottrell, L., Griffin, R., Takami, a., Miyoshi, T., Hatakeyama, S., Shimono, A., Sun, J. Y., Zhang, Y. M., Dzepina, K., Kimmel, J. R., Sueper, D., Jayne, J. T., Herndon, S. C., Trimborn, a. M., Williams, L. R., Wood, E. C., Middlebrook, A. M., Kolb, C. E., Baltensperger, U., Worsnop, D. R., Dunlea, E. J., Huffman, J. A., Onasch, T. B., Alfarra, M. R., Williams, P. I., Bower, K., Kondo, Y., Schneider, J., Drewnick, F., Borrmann, S., Weimer, S., Demerjian, K., Salcedo, D., Cottrell, L., Griffin, R., Takami, a., Miyoshi, T., Hatakeyama, S., Shimono, A., Sun, J. Y., Zhang, Y. M., Dzepina, K., Kimmel, J. R., Sueper, D., Jayne, J. T., Herndon, S. C., Trimborn, a. M., Williams, L. R., Wood, E. C., Middlebrook, A. M., Kolb, C. E., Baltensperger, U., Worsnop, D. R., Dunlea, J., Huffman, J. A., et al.: Evolution of Organic Aerosols in the Atmosphere, Science (80-.)., 326(5959), 1525–1529, doi:10.1126/science.1180353, 2009.

Kahn, R. A., Gaitley, B. J., Martonchik, J. V., Diner, D. J., Crean, K. A. and Holben, B.: Multiangle Imaging Spectroradiometer (MISR) global aerosol optical depth validation based on 2 years of coincident Aerosol Robotic Network (AERONET) observations, J. Geophys. Res. D Atmos., 110(10), 1–16, doi:10.1029/2004JD004706, 2005.

Kim, P. S., Jacob, D. J., Fisher, J. A., Travis, K., Yu, K., Zhu, L., Yantosca, R. M., Sulprizio, M. P., Jimenez, J. L., Campuzano-Jost, P., Froyd, K. D., Liao, J., Hair, J. W., Fenn, M. A., Butler, C. F., Wagner, N. L., Gordon, T. D., Welti, A., Wennberg, P. O., Crounse, J. D., St. Clair, J. M., Teng, A. P., Millet, D. B., Schwarz, J. P., Markovic, M. Z. and Perring, A. E.: Sources, seasonality, and trends of southeast US aerosol: An integrated analysis of surface, aircraft, and satellite observations with the GEOS-Chem chemical transport model, Atmos. Chem. Phys., 15(18), 10411–10433, doi:10.5194/acp-15-10411-2015, 2015.

Koepke, P., Hess, M., Schult, I. and Shettle, E. P.: Global Aerosol Data Set., 1997.

Kreidenweis, S. M., Petters, M. D. and DeMott, P. J.: Single-parameter estimates of aerosol water content, Environ. Res. Lett., 3(3), 035002, doi:10.1088/1748-9326/3/3/035002, 2008.

Levin, E. J. T., Kreidenweis, S. M., McMeeking, G. R., Carrico, C. M., Collett, J. L. and Malm, W. C.: Aerosol physical, chemical and optical properties during the Rocky Mountain Airborne Nitrogen and Sulfur study, Atmos. Environ., 43(11), 1932–1939, doi:10.1016/j.atmosenv.2008.12.042, 2009.

Li, Y., Henze, D. K., Jack, D. and Kinney, P. L.: The influence of air quality model resolution on health impact assessment for fine particulate matter and its components, Air Qual. Atmos. Heal., 9(1), 51–68, doi:10.1007/s11869-015-0321-z, 2016.

Lowenthal, D. and Kumar, N.: Light scattering from sea-salt aerosols at interagency monitoring of protected visual environments (IMPROVE) sites, J. Air Waste Manag., 56(5), 636–642, doi:10.1080/10473289.2006.10464478, 2006.

Malm, C., Sisler, J. F. and Cahill, A.: Spatial and seasonal trends in particle concentration and optical extinction in the United States, , 99, 1347–1370, 1994.

Malm, W. C.: Spatial and monthly trends in speciated fine particle concentration in the United States, J. Geophys. Res., 109(D3), D03306, doi:10.1029/2003JD003739, 2004.

Malm, W. C. and Hand, J. L.: An examination of the physical and optical properties of aerosols collected in the IMPROVE program, Atmos. Environ., 41(16), 3407–3427, doi:10.1016/j.atmosenv.2006.12.012, 2007.

Malm, W. C. and Kreidenweis, S. M.: The effects of models of aerosol hygroscopicity on the apportionment of extinction, Atmos. Environ., 31(13), 1965–1976, doi:10.1016/S1352-2310(96)00355-X, 1997.

Mann, G. W., Carslaw, K. S., Spracklen, D. V., Ridley, D. A., Manktelow, P. T., Chipperfield, M. P., Pickering, S. J. and Johnson, C. E.: Description and evaluation of GLOMAP-mode: A modal global aerosol microphysics model for the UKCA composition-climate model, Geosci. Model Dev., 3(2), 519–551, doi:10.5194/gmd-3-519-2010, 2010.

Marais, E. A., Jacob, D. J., Jimenez, J. L., Campuzano-Jost, P., Day, D. A., Hu, W., Krechmer, J., Zhu, L., Kim, P. S., Miller, C. C., Fisher, J. A., Travis, K., Yu, K., Hanisco, T. F., Wolfe, G. M., Arkinson, H. L., Pye, H. O. T., Froyd, K. D., Liao, J. and McNeill, V. F.: Aqueous-phase mechanism for secondary organic aerosol formation from isoprene: Application to the southeast United States and co-benefit of SO2 emission controls, Atmos. Chem. Phys., 16(3), 1603–1618, doi:10.5194/acp-16-1603-2016, 2016.

Martin, R. V.: Global and regional decreases in tropospheric oxidants from photochemical effects of aerosols, J. Geophys. Res., 108(D3), 4097, doi:10.1029/2002JD002622, 2003.

Martin, S. T., Schlenker, J. C., Malinowski, A. and Hung, H.: Crystallization of atmospheric sulfate-nitrate-ammonium particles, , 30(21), 1–4, doi:10.1029/2003GL017930, 2003.

Martin, S. T., Rosenoern, T., Chen, Q. and Collins, D. R.: Phase changes of ambient particles in the Southern Great Plains of Oklahoma, Geophys. Res. Lett., 35(22), 1–5, doi:10.1029/2008GL035650, 2008.

Mishchenko, M. I., Dlugach, J. M., Yanovitskij, E. G. and Zakharova, N. T.: Bidirectional reflectance of flat, optically thick particulate layers: An efficient radiative transfer solution and applications to snow and soil surfaces, J. Quant. Spectrosc. Radiat. Transf., 63(2–6), 409–432, doi:10.1016/S0022-4073(99)00028-X, 1999.

Molenar, J. V: Analysis of the Real World Performance of the Optec NGN-2 Ambient Nephelometer, Vis. Air Qual. Aerosols Glob. Radiat. Balanc., 243–265, 1997.

Ng, N. L., Canagaratna, M. R., Zhang, Q., Jimenez, J. L., Tian, J., Ulbrich, I. M., Kroll, J. H., Docherty, K. S., Chhabra, P. S., Bahreini, R., Murphy, S. M., Seinfeld, J. H., Hildebrandt, L., Donahue, N. M., Decarlo, P. F., Lanz, V. A., Prévôt, A. S. H., Dinar, E., Rudich, Y. and Worsnop, D. R.: Organic aerosol components observed in Northern Hemispheric datasets from Aerosol Mass Spectrometry, Atmos. Chem. Phys., 10(10), 4625–4641, doi:10.5194/acp-10-4625-2010, 2010.

Pandolfi, M., Alados-arboledas, L., Andrade, M., Backman, J., Baltensperger, U., Bonasoni, P., Bukowiecki, N., Coen, C., Conil, S., Coz, E., Crenn, V., Dudoitis, V., Eleftheriadis, K., Favez, O., Fetfatzis, P., Fiebig, M., Ginot, P., Gysel, M., Henzing, B., Hoffer, A., Holubova, A., Kalapov, I., Kalivitis, N., Kouvarakis, G., Kristensson, A., Kulmala, M., Lihavainen, H., Lunder, C., Luoma, K., Lyamani, H., Mihalopoulos, N., Moerman, M., Dowd, C. O., Petit, J., Pichon, J. M., Prokopciuk, N., Putaud, J., Sciare, J., Sellegri, K., Stamenov, D. B., Swietlicki, E., Titos, G., Tuch, T., Tunved, P., Ulevicius, V., Vaishya, A., Virkkula, A., Vratolis, S., Weingartner, E., Wiedensohler, A. and Laj, P.: Discussion started : 13 October 2017 Manuscript under review for journal Atmos . Chem . Phys . Discussion started : 13 October 2017 c Author (s) 2017 . CC BY 4 . 0 License ., , (October), 2017.

Park, R. J.: Sources of carbonaceous aerosols over the United States and implications for natural visibility, J. Geophys. Res., 108(D12), 4355, doi:10.1029/2002JD003190, 2003.

Park, R. J., Jacob, D. J., Field, B. D., Yantosca, R. M. and Chin, M.: Natural and transboundary pollution influences on sulfate-nitrate-ammonium aerosols in the United States: Implications for policy, J. Geophys. Res. D Atmos., 109(15), doi:10.1029/2003JD00473, 2004.

Petters, M. D. and Kreidenweis, S. M.: A single parameter representation of hygroscopic growth and cloud\ncondensation nucleus activity, Atmos. Chem. Phys., 1961–1971, doi:10.5194/acp-7-1961-2007, 2007.

Petters, M. D. and Kreidenweis, S. M.: A single parameter representation of hygroscopic growth and cloud condensation nucleus activity-Part 3: Including surfactant partitioning, Atmos. Chem. Phys., 13(2), 1081–1091, doi:10.5194/acp-13-1081-2013, 2013.

Philip, S., Martin, R. V, van Donkelaar, A., Lo, J. W.-H., Wang, Y., Chen, D., Zhang, L., Kasibhatla, P. S., Wang, S., Zhang, Q., Lu, Z., Streets, D. G., Bittman, S. and Macdonald, D. J.: Global Chemical Composition of Ambient Fine Particulate Matter for Exposure Assessment, Environ. Sci. Technol., 48(22), 13060–13068, doi:10.1021/es502965b, 2014a.

Philip, S., Martin, R. V., Pierce, J. R., Jimenez, J. L., Zhang, Q., Canagaratna, M. R., Spracklen, D. V., Nowlan, C. R., Lamsal, L. N., Cooper, M. J. and Krotkov, N. A.: Spatially and seasonally resolved estimate of the ratio of organic mass to organic carbon, Atmos. Environ., 87, 34–40, doi:10.1016/j.atmosenv.2013.11.065, 2014b.

Pye, H. O. T., Liao, H., Wu, S., Mickley, L. J., Jacob, D. J., Henze, D. J. and Seinfeld, J. H.: Effect of changes in climate and emissions on future sulfate-nitrate-ammonium aerosol levels in the United States, J. Geophys. Res. Atmos., 114(1), 1–18, doi:10.1029/2008JD010701, 2009.

Pye, H. O. T., Chan, A. W. H., Barkley, M. P. and Seinfeld, J. H.: Global modeling of organic aerosol: The importance of reactive nitrogen (NOx and NO3), Atmos. Chem. Phys., 10(22), 11261–11276, doi:10.5194/acp-10-11261-2010, 2010.

Rickards, A. M. J., Miles, R. E. H., Davies, J. F., Marshall, F. H. and Reid, J. P.: Measurements of the sensitivity of aerosol hygroscopicity and the κ parameter to the O/C ratio, J. Phys. Chem. A, 117(51), 14120–14131, doi:10.1021/jp407991n, 2013.

Ridley, D. A., Heald, C. L. and Ford, B.: North African dust export and deposition: A satellite and model perspective, J. Geophys. Res. Atmos., 117(2), 1–21, doi:10.1029/2011JD016794, 2012.

Ridley, D. A., Heald, C. L., Ridley, K. J. and Kroll, J. H.: Causes and consequences of decreasing atmospheric organic aerosol in the United States, Proc. Natl. Acad. Sci., 201700387, doi:10.1073/pnas.1700387115, 2017.

Singh, H. B., Brune, W. H., Crawford, J. H., Jacob, D. J. and Russell, P. B.: Overview of the summer 2004 Intercontinental Chemical Transport Experiment-North America (INTEX-A), J. Geophys. Res. Atmos., 111(24), doi:10.1029/2006JD007905, 2006.

Snider, G., Weagle, C. L., Martin, R. V., Van Donkelaar, A., Conrad, K., Cunningham, D., Gordon, C., Zwicker, M., Akoshile, C., Artaxo, P., Anh, N. X., Brook, J., Dong, J., Garland, R. M., Greenwald, R., Griffith, D., He, K., Holben, B. N., Kahn, R., Koren, I., Lagrosas, N., Lestari, P., Ma, Z., Vanderlei Martins, J., Quel, E. J., Rudich, Y., Salam, A., Tripathi, S. N., Yu, C., Zhang, Q., Zhang, Y., Brauer, M., Cohen, A., Gibson, M. D. and Liu, Y.: SPARTAN: A global network to evaluate and enhance satellite-based estimates of ground-level particulate matter for global health applications, Atmos. Meas. Tech., 8(1), 505–521, doi:10.5194/amt-8-505-2015, 2015.

Snider, G., Weagle, C. L., Murdymootoo, K. K., Ring, A., Ritchie, Y., Stone, E., Walsh, A., Akoshile, C., Anh, N. X., Balasubramanian, R., Brook, J., Qonitan, F. D., Dong, J., Griffith, D., He, K., Holben, B. N., Kahn, R., Lagrosas, N., Lestari, P., Ma, Z., Misra, A., Norford, L. K., Quel, E. J., Salam, A., Schichtel, B., Segev, L., Tripathi, S., Wang, C., Yu, C., Zhang, Q., Zhang, Y., Brauer, M., Cohen, A., Gibson, M. D., Liu, Y., Martins, J. V., Rudich, Y. and Martin, R. V.: Variation in global chemical composition of PM2.5: emerging results from SPARTAN, Atmos. Chem. Phys., 16(15), 9629–9653, doi:10.5194/acp-16-9629-2016, 2016.

Solomon, P. A., Crumpler, D., Flanagan, J. B., Jayanty, R. K. M., Rickman, E. E. and McDade, C. E.: U.S. National PM2.5 Chemical Speciation Monitoring Networks-CSN and IMPROVE: Description of Networks., J. Air Waste Manage. Assoc., 64(12), 1410–38, doi:10.1080/10962247.2014.956904, 2014.

Spracklen, D. V., Pringle, K. J., Carslaw, K. S., Chipperfield, M. P. and Mann, G. W.: A global off-line model of size-resolved aerosol microphysics: I. Model development and prediction of aerosol properties, Atmos. Chem. Phys., 5(8), 2227–2252, doi:10.5194/acp-5-2227-2005, 2005.

Stanier, C. O., Khlystov, A. Y. and Pandis, S. N.: Ambient aerosol size distributions and number concentrations measured during the Pittsburgh Air Quality Study (PAQS), Atmos. Environ., 38(20), 3275–3284, doi:10.1016/j.atmosenv.2004.03.020, 2004.

Tao, J., Zhang, L., Ho, K., Zhang, R., Lin, Z., Zhang, Z., Lin, M., Cao, J., Liu, S. and Wang, G.: Impact of PM 2 . 5 chemical compositions on aerosol light scattering in Guangzhou — the largest megacity in South China, Atmos. Res., 135–136, 48–58, doi:10.1016/j.atmosres.2013.08.015, 2014.

Titos, G., Foyo-Moreno, I., Lyamani, H., Querol, X., Alastuey, A. and Alados-Arboledas, L.: Optical properties and chemical composition of aerosol particles at an urban location: An estimation of the aerosol mass scattering and absorption efficiencies, J. Geophys. Res. Atmos., 117(4), 1–12, doi:10.1029/2011JD016671, 2012.

Trivitayanurak, W., Adams, P. J., Spracklen, D. V. and Carslaw, K. S.: Tropospheric aerosol microphysics simulation with assimilated meteorology: Model description and intermodel comparison, Atmos. Chem. Phys., 8(12), 3149–3168, doi:10.5194/acp-8-3149-2008, 2008.

Wang, J., Hoffmann, A. A., Park, R. J., Jacob, D. J. and Martin, S. T.: Global distribution of solid and aqueous sulfafte aerosols: Effect of the hysteresis of particle phase transitions, J. Geophys. Res. Atmos., 113(11), 1–11, doi:10.1029/2007JD009367, 2008.

Wang, Q., Jacob, D. J., Spackman, J. R., Perring, A. E., Schwarz, J. P., Moteki, N., Marais, E. A., Ge, C., Wang, J. and Barrett, S. R. H.: Global budget and radiative forcing of black carbon aerosol : Constraints from pole-to-pole (HIPPO) observations across the Pacific, , 119, 195–206, doi:10.1002/2013JD020824, 2014.

Wexler, A. S. and Clegg, S. L.: Atmospheric aerosol models for systems including the ions H + , NH 4 + , Na + , SO 4 2− , NO 3 − , Cl − , Br − , and H 2 O, J. Geophys. Res., 107(D14), 4207, doi:10.1029/2001JD000451, 2002.

White, W. H.: On the theoretical and empirical basis for apportioning extinction by aerosols: A critical review, Atmos. Environ., 20(9), 1659–1672, doi:10.1016/0004-6981(86)90113-7, 1986.

White, W. H., Macias, E. S., Nininger, R. C. and Schorran, D.: Size-resolved measurements of light scattering by ambient particles in the southwestern U.S.A., Atmos. Environ., 28(5), 909–921, doi:10.1016/1352-2310(94)90249-6, 1994.

Wise, M. E.: Hygroscopic growth of ammonium sulfate/dicarboxylic acids, J. Geophys. Res., 108(D20), 4638, doi:10.1029/2003JD003775, 2003.

Yu, F. and Luo, G.: Simulation of particle size distribution with a global aerosol model: Contribution of nucleation to aerosol and CCN number concentrations, Atmos. Chem. Phys., 9(20), 7691–7710, doi:10.5194/acp-9-7691-2009, 2009.

Zhang, L., Kok, J. F., Henze, D. K., Li, Q. and Zhao, C.: Improving simulations of fine dust surface concentrations over the western United States by optimizing the particle size distribution, Geophys. Res. Lett., 40(12), 3270–3275, doi:10.1002/grl.50591, 2013.

Formatted: Normal, No widow/orphan control, Don't adjust space between Latin and Asian text, Don't adjust space between Asian text and numbers

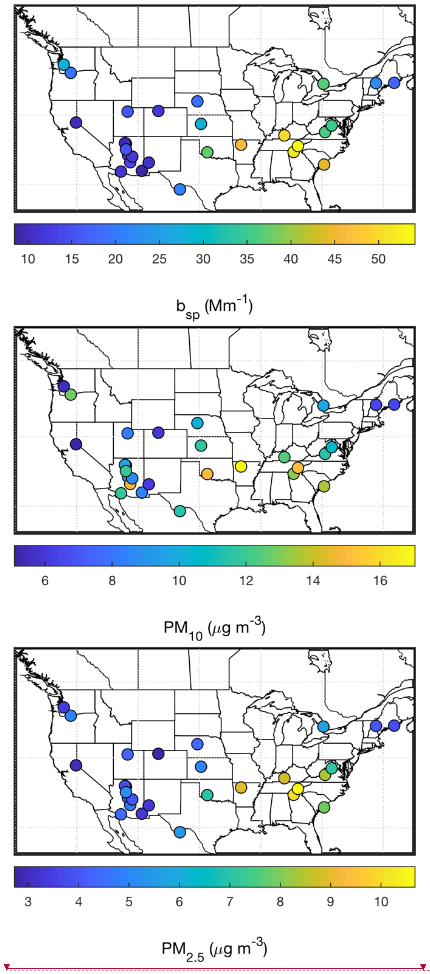

Figure 1: Map of IMPROVE sites with collocated scatter (b_{sp}) at 550 nm and ambient relative humidity, PM_{10} and $PM_{2.5}$ measurements in North America between 2000-2010

Deleted: ... [1]

Formatted: Left

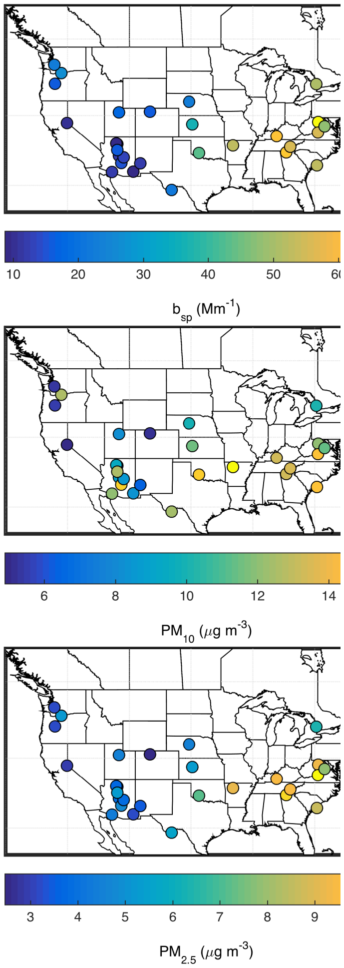

Deleted:

Deleted: 5

Deleted: **Overlaying circles represent average collocated b_{sp} (top), PM_{10} (middle) and $PM_{2.5}$ (bottom).**

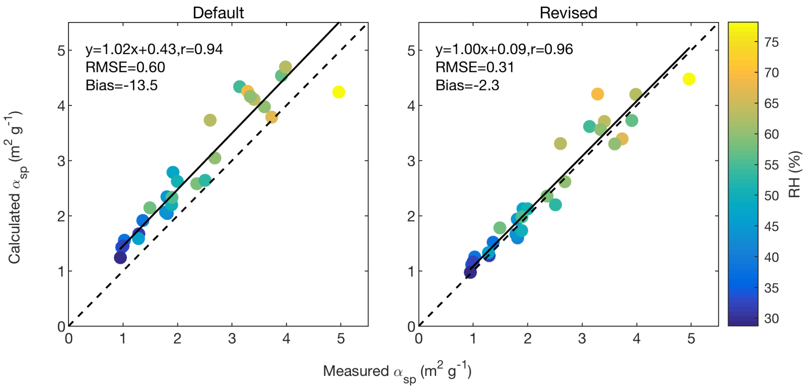

Figure 2: Average measured vs calculated α_{sp} at 550 nm at IMPROVE sites between 2000-2010 using GEOS-Chem default optical tables and revised optical tables. The colour of each point corresponds to the average relative humidity at the site. The 1:1 line is black. Slope, offset and correlation coefficient are inset.

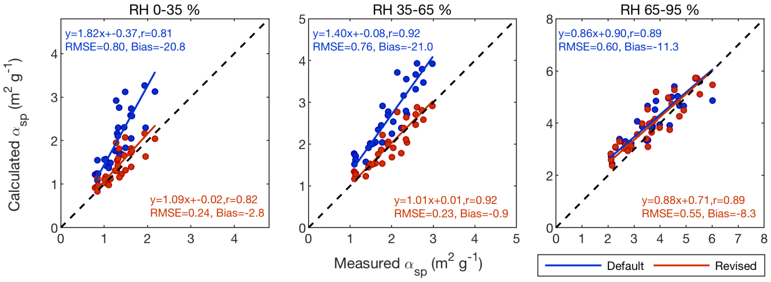

Figure 3: Average measured versus calculated α_{sp} at 550 nm at IMPROVE sites between 2000-2010 using GEOS-Chem default and revised optical tables (Table A1) for measurements taken in 0-35 % RH, 35-65 % RH and 65-95 % RH conditions. The 1:1 line is black. Slope, offset and correlation coefficient are inset.

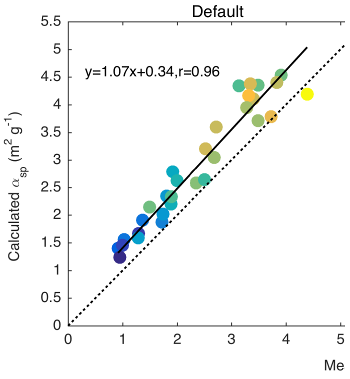

Deleted:

Formatted: Caption

Deleted: color

Deleted: ... [2]

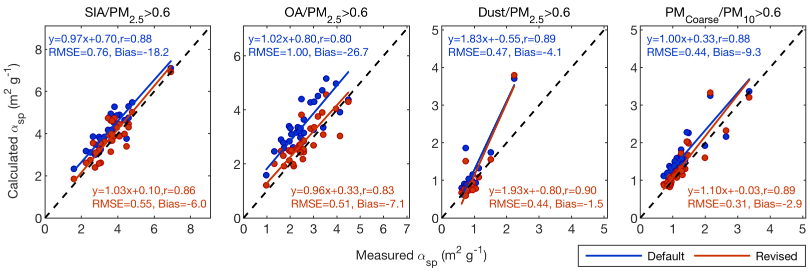

Figure 4: Average measured versus calculated α_{sp} (550 nm) at IMPROVE sites between 2000-2010 using GEOS-Chem default and revised optical tables for measurements taken in conditions dominated by secondary inorganic aerosols (SIA), organic aerosols (OA), fine dust, and PM$_{coarse}$ (PM$_{10}$-PM$_{2.5}$). The 1:1 line is black. Slope, offset, and correlation coefficient are inset.

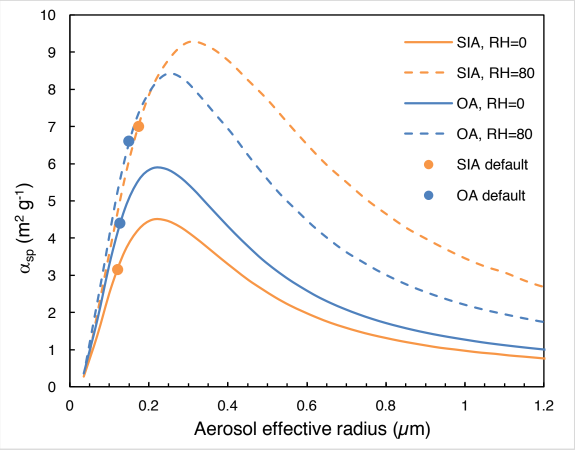

Figure 5: Mass scattering efficiency (α_{sp}) at 550 nm as a function of aerosol wet effective radius for organic aerosol and secondary inorganic aerosol. Solid lines show α_{sp} for dry aerosol (RH=0%), dashed lines show α_{sp} for aqueous aerosols (RH=80%). Points represent the default size in GEOS-Chem.

Deleted:

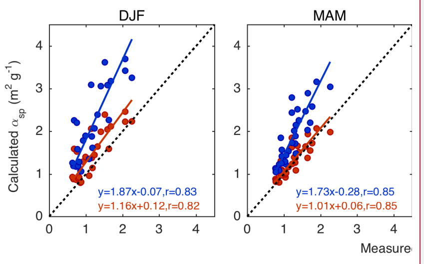

Deleted:

Deleted: **Figure 4: Average measured versus calculated α_{sp} at IMPROVE sites using GEOS-Chem default and revised optical tables using measurements taken in SIA dominant conditions, OA dominated conditions, Dust dominant conditions and PM$_{coarse}$ dominated conditions. The 1:1 line is black. Slope, offset and correlation coefficient are inset.**

Deleted: ... [3]

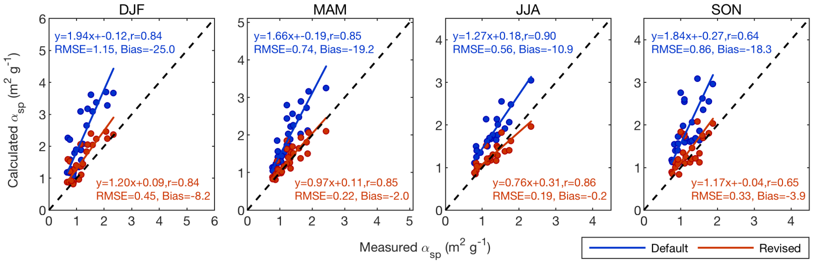

Figure 6: Average measured versus calculated α_{sp} (550 nm) at IMPROVE sites between 2000-2010 using GEOS-Chem default and revised optical tables for measurements taken in dry conditions (RH<35 %) in winter, spring, summer and fall. The 1:1 line is black. Slope, offset and correlation coefficient are inset.

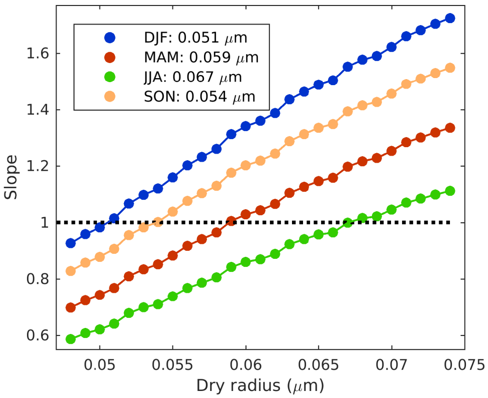

Figure 7: Slope of measured vs. calculated α_{sp} plot versus dry geometric mean aerosol radius, by season. Winter (DJF) is in blue, spring (MAM) in red, summer (JJA) in green and fall (SON) in orange. The line Slope=1 is shown in black. Numbers in the legend represent the dry radius for which slope=1 for each season.

Formatted: Normal

Deleted:

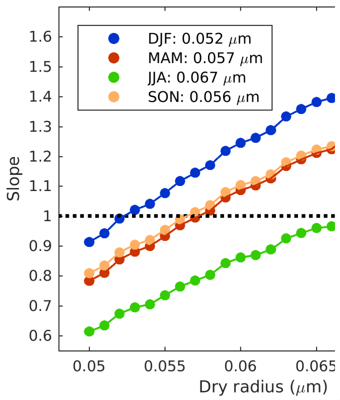

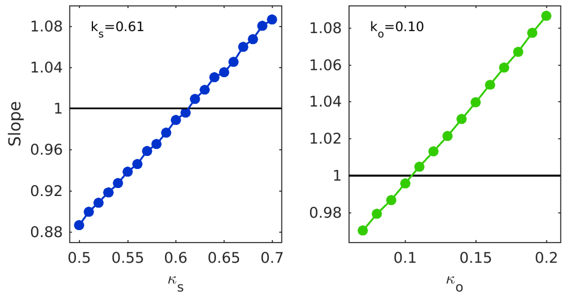

Figure 8: Slope of measured vs. calculated α_{sp} plot as a function of the κ of secondary inorganic aerosols (κ_S, left) and the κ of organic aerosols (κ_O, right). The line slope=1 is shown in black. κ_s and κ_o values for which slope=1 are inset.

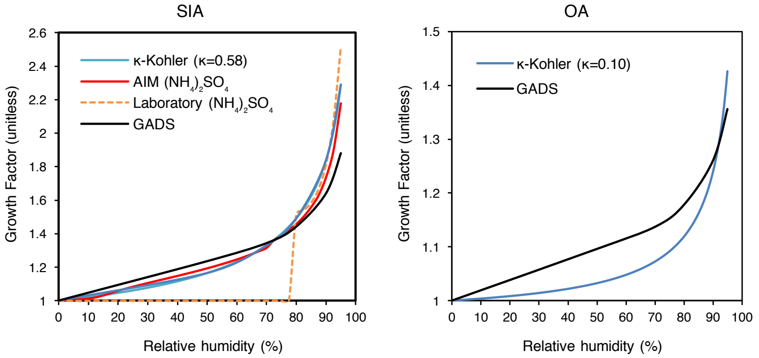

Figure 9: Hygroscopic growth factor curves for secondary inorganic aerosols (SIA, left) and organic aerosols (OA, right). GADS (Global Aerosol Data Set) hygroscopic growth from empirical data and κ-Kohler hygroscopic growth are shown for both SIA and OA. For ammonium sulfate, AIM (Aerosol Inorganic Model) hygroscopic growth at T=298 K (Wexler and Clegg, 2002) and laboratory hygroscopic growth with a deliquesence point of RH=80 % (Wise et al., 2003) are also shown.

Deleted: s

Formatted: Not Superscript/ Subscript

Deleted: (

Deleted: o

Deleted: (

Deleted: SIA

Deleted: (

Deleted: (

Formatted: Font:Bold

Deleted: (Wexler and Clegg, 2002)

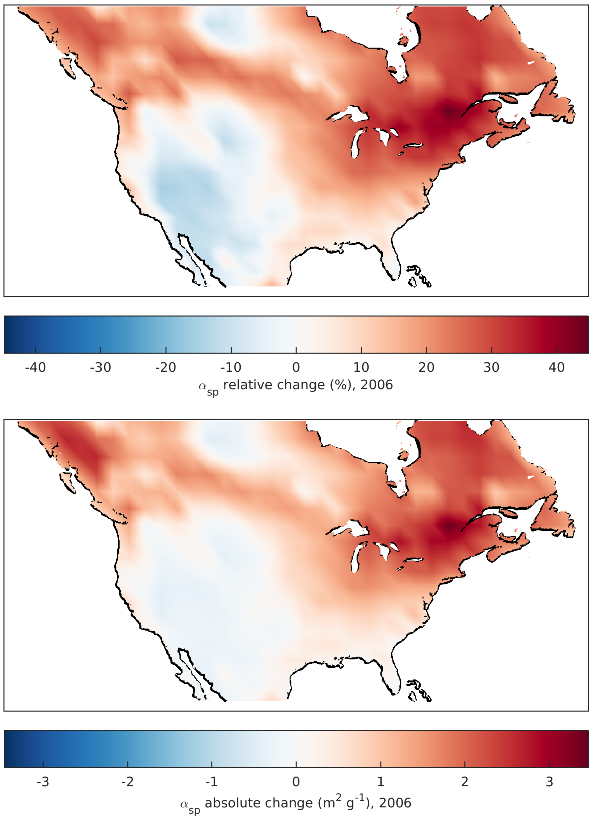

Figure 10: Average relative and absolute change in GEOS-Chem mass scattering efficiency over North America for the year 2006 after implementing revised optical tables for secondary inorganic and organic aerosols.

Deleted: ... [4]

Deleted: **SIA and OA**

Deleted:

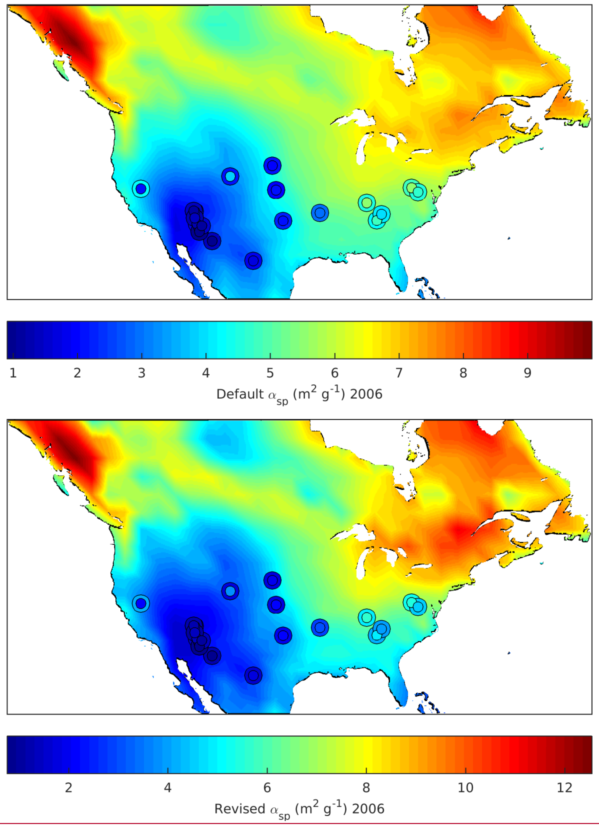

Figure 11: GEOS-Chem annual average mass scattering efficiency (at 550 nm) for the year 2006 using default and revised size and hygroscopicity for secondary inorganic and organic aerosols. Overlaying inner circles represent annual averages of α_{sp} at IMPROVE network sites for the year 2006. Outer rings represent coincident average simulated α_{sp}.

Deleted: SIA and OA

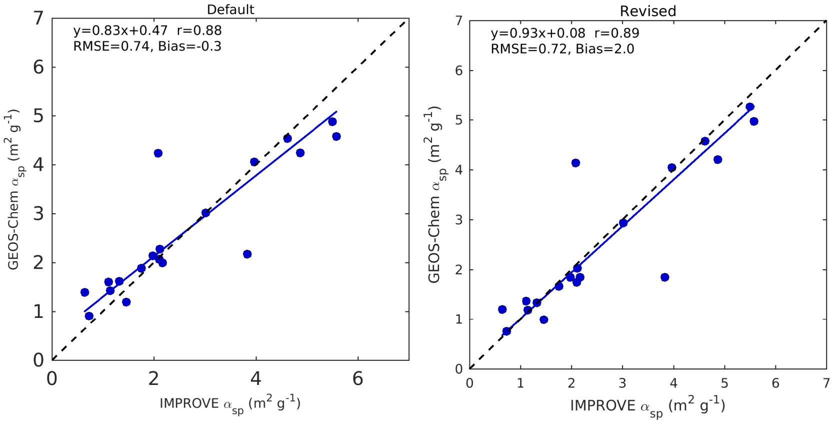

Figure 12: Coincident simulated versus measured average mass scattering efficiency at 550 nm for the year 2006, using default and revised optical tables. Slope, offset and correlation coefficient are inset.

Deleted:

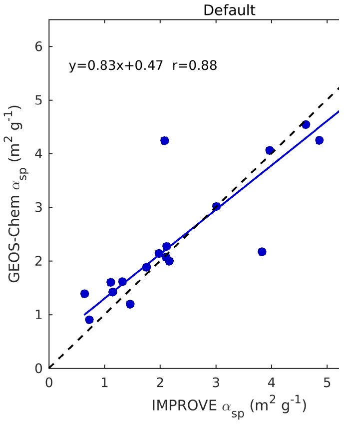

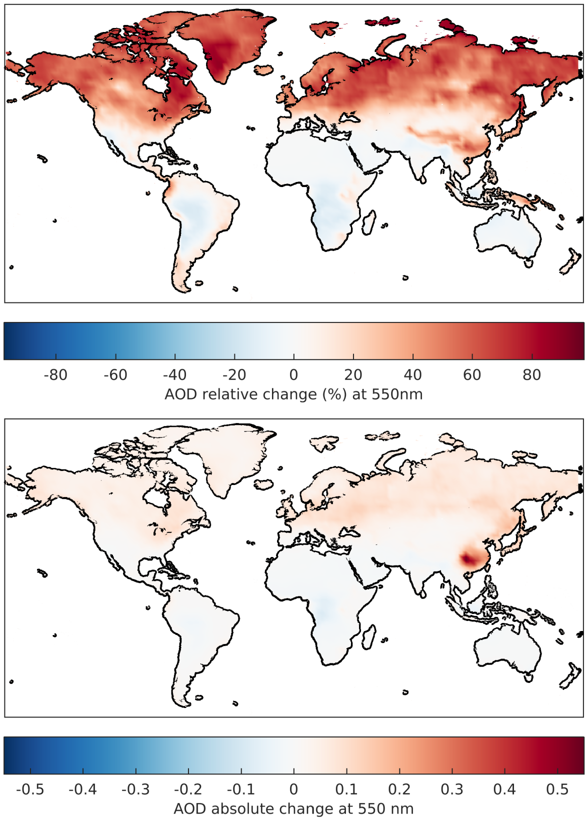

Figure B1: Average relative and absolute change in GEOS-Chem aerosol optical depth at 550 nm globally for the year 2006 after implementing revised optical tables for SIA and OA.

Deleted: ... [5]

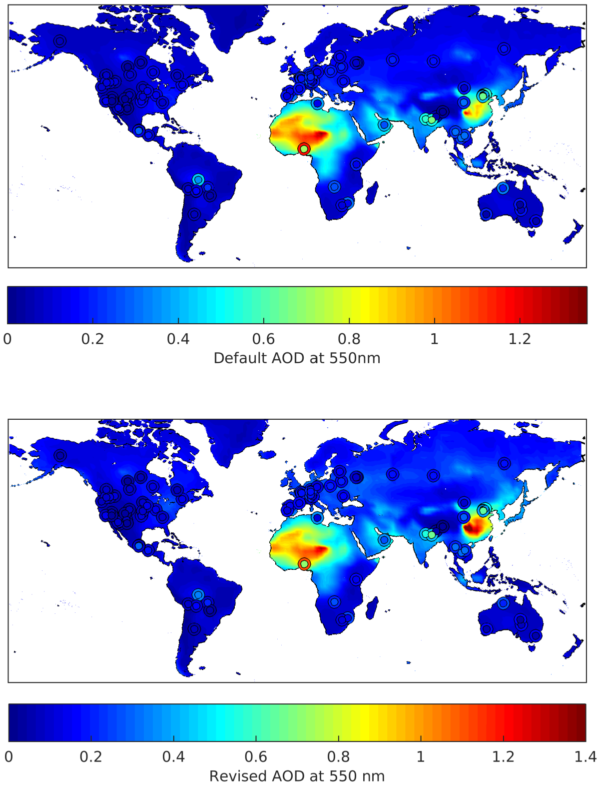

Figure B2: Global comparison for the year 2006 of AERONET AOD (inner circles) and GEOS-Chem coincident simulated AOD (outer rings) using default optical tables.

Deleted:

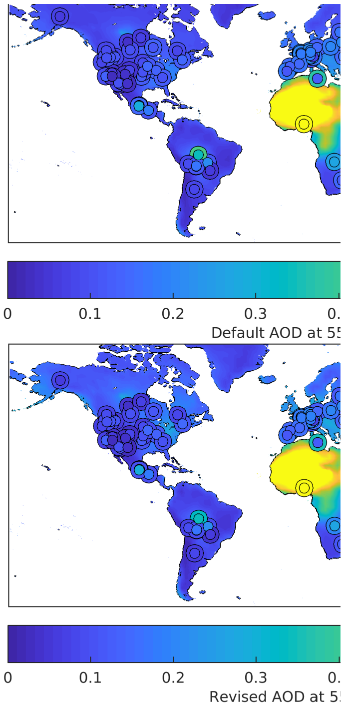

Deleted:

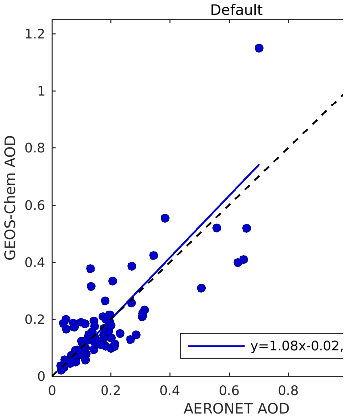

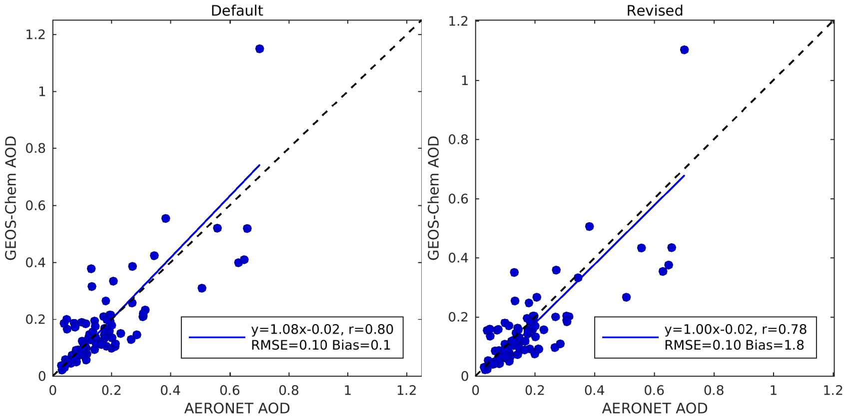

Figure B.3 Coincident simulated versus measured AOD at 550 nm at AERONET sites for the year 2006, using default and revised sizes and hygroscopicity. Slope, offset and correlation coefficient are inset. The 1:1 line is shown in black.

Aerosol	RH	Default				Revised (κ_S=0.61, κ_O=0.10)			
		r_g (μm)	r_{eff} (μm)	Q	SSA	r_g (μm)	r_{eff} (μm)	Q	SSA
SIA	0	0.069	0.121	0.902	0.965	0.058	0.101	0.603	0.959
	35	0.081	0.141	0.965	0.975	0.064	0.111	0.629	0.967
	50	0.086	0.149	0.992	0.979	0.068	0.118	0.656	0.972
	70	0.093	0.163	1.062	0.983	0.078	0.135	0.742	0.981
	80	0.100	0.174	1.137	0.986	0.088	0.152	0.847	0.987
	90	0.114	0.198	1.301	0.991	0.108	0.188	1.116	0.993
	95	0.131	0.227	1.517	0.994	0.135	0.234	1.500	0.997
	99	0.175	0.304	1.272	0.993	0.229	0.397	2.570	0.999
OA	0	0.073	0.127	1.007	0.966	0.058	0.101	0.603	0.959
	35	0.078	0.135	0.965	0.972	0.059	0.103	0.608	0.965
	50	0.080	0.139	0.947	0.975	0.060	0.104	0.610	0.963
	70	0.083	0.145	0.947	0.978	0.063	0.108	0.622	0.966
	80	0.086	0.149	0.955	0.980	0.065	0.113	0.639	0.970
	90	0.092	0.159	0.990	0.984	0.073	0.125	0.696	0.977
	95	0.099	0.171	1.053	0.988	0.084	0.144	0.811	0.985
	99	0.117	0.203	1.273	0.993	0.132	0.223	1.463	0.996

Table A1: Default and revised aerosol size and optical properties for secondary inorganic aerosols (SIA) and organic aerosols (OA) at 550 nm at 8 relative humidity values. Columns indicate geometric mean radius (r_g), effective radius (r_{eff}), extinction efficiency (Q), and single scattering albedo (SSA). κ_s and κ_o represent the hygroscopic growth parameters for SIA and OA, respectively.

Deleted: s

Deleted: 58

Deleted: o

Deleted: 0.065

Deleted: 0.112

Deleted: 0.638

Deleted: 0.968

Deleted: 7

Deleted: 3

Deleted: 7

Deleted: 4

Deleted: 34

Deleted: 0

Deleted: 7

Deleted: 0

Deleted: 35

Deleted: 6

Deleted: 7

Deleted: 5

Deleted: 095

Deleted: 3

Deleted: 1

Deleted: 470

Deleted: 6

Deleted: 5

Deleted: 1

Deleted: 41

Component	r_g (μm)	σ	ρ_d (g/cm^3)
Sulfate/Nitrate/Ammonium	0.070	1.6	1.7
Organic Carbon	0.073	1.6	1.3
Black Carbon	0.020	1.6	1.8
Sea-salt (fine)	0.085	1.5	2.2
Sea-salt (coarse)	0.401	1.8	2.2
Brown Carbon	0.073	1.6	1.3
Dust 1 a-d	0.030-0.170	2.2	2.5
Dust 2	0.265	2.2	2.65
Dust 3	0.530	2.2	2.65
Dust 4	0.845	2.2	2.65

Deleted: ... [6]

Table A2: Current microphysical properties of each aerosol species in GEOS-Chem. r_g represents the dry geometric mean radius (μm) and σ the geometric standard deviation of the lognormal size distributions assumed for each species. ρ_d represents the dry mass densities of each species (g/cm^3).

Page 38: [1] Deleted Robyn Latimer 10/23/18 1:09:00 PM

Andrews, E., Ogren, J. A., Bonasoni, P., Marinoni, A., Cuevas, E., Rodríguez, S., Sun, J. Y., Jaffe, D. A., Fischer, E. V., Baltensperger, U., Weingartner, E., Coen, M. C., Sharma, S., Macdonald, A. M., Leaitch, W. R., Lin, N. H., Laj, P., Arsov, T., Kalapov, I., Jefferson, A. and Sheridan, P.: Climatology of aerosol radiative properties in the free troposphere, Atmos. Res., 102(4), 365–393, doi:10.1016/j.atmosres.2011.08.017, 2011.

Bey, I., Jacob, D. J., Yantosca, R. M., Logan, J. A., Field, B. D., Fiore, A. M., Li, Q.-B., Liu, H.-Y., Mickley, L. J. and Schultz, M. G.: Global Modeling of Tropospheric Chemistry with Assimilated Meteorology: Model Description and Evaluation, J. Geophys. Res., 106, 73–95, doi:10.1029/2001JD000807, 2001.

Chin, M., Ginoux, P., Kinne, S., Torres, O., Holben, B. N., Duncan, B. N., Martin, R. V., Logan, J. a., Higurashi, A. and Nakajima, T.: Tropospheric Aerosol Optical Thickness from the GOCART Model and Comparisons with Satellite and Sun Photometer Measurements, J. Atmos. Sci., 59(3), 461–483, doi:10.1175/1520-0469(2002)059<0461:TAOTFT>2.0.CO;2, 2002.

Ciobanu, V. G., Marcolli, C., Krieger, U. K., Zuend, A. and Peter, T.: Efflorescence of ammonium sulfate and coated ammonium sulfate particles: Evidence for surface nucleation, J. Phys. Chem. A, 114(35), 9486–9495, doi:10.1021/jp103541w, 2010.

Collaud Coen, M., Andrews, E., Asmi, A., Baltensperger, U., Bukowiecki, N., Day, D., Fiebig, M., Fjaeraa, A. M., Flentje, H., Hyvärinen, A., Jefferson, A., Jennings, S. G., Kouvarakis, G., Lihavainen, H., Lund Myhre, C., Malm, W. C., Mihapopoulos, N., Molenar, J. V., O'Dowd, C., Ogren, J. A., Schichtel, B. A., Sheridan, P., Virkkula, A., Weingartner, E., Weller, R. and Laj, P.: Aerosol decadal trends-Part 1: In-situ optical measurements at GAW and IMPROVE stations, Atmos. Chem. Phys., 13(2), 869–894, doi:10.5194/acp-13-869-2013, 2013.

van Donkelaar, A., Martin, R. V., Brauer, M., Kahn, R., Levy, R., Verduzco, C. and Villeneuve, P. J.: Global estimates of ambient fine particulate matter concentrations from satellite-based aerosol optical depth: Development and application, Environ. Health Perspect., 118(6), 847–855, doi:10.1289/ehp.0901623, 2010.

Dougle, P. G., Veefkind, J. P. and R, H. M. B.: Crystallisation of mixtures of ammonium nitrate, ammonium sulphate and soot, , 29(3), 375–386, 1998.

Drury, E., Jacob, D. J., Spurr, R. J. D., Wang, J., Shinozuka, Y., Anderson, B. E., Clarke, A. D., Dibb, J., McNaughton, C. and Weber, R.: Synthesis of satellite (MODIS), aircraft (ICARTT), and surface (IMPROVE, EPA-AQS, AERONET) aerosol observations over eastern North America to improve MODIS aerosol retrievals and constrain surface aerosol concentrations and sources, J. Geophys. Res. Atmos., 115(14), 1–17, doi:10.1029/2009JD012629, 2010.

Duplissy, J., De Carlo, P. F., Dommen, J., Alfarra, M. R., Metzger, A., Barmpadimos, I., Prevot, A. S. H., Weingartner, E., Tritscher, T., Gysel, M., Aiken, A. C., Jimenez, J. L., Canagaratna, M. R., Worsnop, D. R., Collins, D. R., Tomlinson, J. and Baltensperger, U.: Relating hygroscopicity and composition of organic aerosol particulate matter, Atmos. Chem. Phys., 11(3), 1155–1165, doi:10.5194/acp-11-1155-2011, 2011.

Dusek, U., Frank, G. P., Massling, A., Zeromskiene, K., Iinuma, Y., Schmid, O., Helas, G., Hennig, T., Wiedensohler, A. and Andreae, M. O.: Water uptake by biomass burning aerosol at sub-and supersaturated conditions: Closure studies and implications for the role of organics, Atmos. Chem. Phys., 11(18), 9519–9532, doi:10.5194/acp-11-9519-2011, 2011.

Fairlie, D. T., Jacob, D. J. and Park, R. J.: The impact of transpacific transport of mineral dust in the United States, Atmos. Environ., 41(6), 1251–1266, doi:10.1016/j.atmosenv.2006.09.048, 2007.

Fairlie, T. D., Jacob, D. J., Dibb, J. E., Alexander, B., Avery, M. A., Van Donkelaar, A. and Zhang, L.: Impact of mineral dust on nitrate, sulfate, and ozone in transpacific Asian pollution plumes, Atmos. Chem. Phys., 10(8), 3999–4012, doi:10.5194/acp-10-3999-2010, 2010.

Fehsenfeld, F. C., Ancellet, G., Bates, T. S., Goldstein, A. H., Hardesty, R. M., Honrath, R., Law, K. S., Lewis, A. C., Leaitch, R., McKeen, S., Meagher, J., Parrish, D. D., Pszenny, A. A. P., Russell, P. B., Schlager, H., Seinfeld, J., Talbot, R. and Zbinden, R.: International Consortium for Atmospheric Research on Transport and Transformation (ICARTT): North America to Europe - Overview of the 2004 summer field study, J. Geophys. Res. Atmos., 111(23), doi:10.1029/2006JD007829, 2006.

Fountoukis, C. and Nenes, A.: ISORROPIA II: a computationally efficient thermodynamic equilibrium model for K –H 2 O aerosols, Atmos. Chem. Phys. Atmos. Chem. Phys., 7, 4639–4659, doi:10.5194/acp-7-4639-2007, 2007.

Gebhart, K. A., Copeland, S. and Malm, W. C.: Diurnal and seasonal patterns in light scattering, extinction, and relative humidity, Atmos. Environ., 35(30), 5177–5191, doi:10.1016/S1352-2310(01)00319-3, 2001.

Hand, J. L. and Malm, W. C.: Review of aerosol mass scattering efficiencies from ground-based measurements since 1990, J. Geophys. Res. Atmos., 112(16), doi:10.1029/2007JD008484, 2007.

Hersey, S. P., Craven, J. S., Metcalf, A. R., Lin, J., Lathem, T., Suski, K. J., Cahill, J. F., Duong, H. T., Sorooshian, A., Jonsson, H. H., Shiraiwa, M., Zuend, A., Nenes, A., Prather, K. A., Flagan, R. C. and Seinfeld, J. H.: Composition and hygroscopicity of the Los Angeles Aerosol: CalNex, J. Geophys. Res. Atmos., 118(7), 3016–3036, doi:10.1002/jgrd.50307, 2013.

Holben, B. N., Eck, T. F., Slutsker, I., Tanré, D., Buis, J. P., Setzer, A., Vermote, E., Reagan, J. A., Kaufman, Y. J., Nakajima, T., Lavenu, F., Jankowiak, I. and Smirnov, A.: AERONET—A Federated Instrument Network and Data Archive for Aerosol Characterization, Remote Sens. Environ., 66(1), 1–16, doi:10.1016/S0034-4257(98)00031-5, 1998.

Hyslop, N. P. and White, W. H.: An evaluation of interagency monitoring of protected visual environments (IMPROVE) collocated precision and uncertainty estimates, Atmos. Environ., 42(11), 2691–2705, doi:10.1016/j.atmosenv.2007.06.053, 2008.

Jaeglé, L., Quinn, P. K., Bates, T. S., Alexander, B. and Lin, J. T.: Global distribution of sea salt aerosols: New constraints from in situ and remote sensing observations, Atmos. Chem. Phys., 11(7), 3137–3157, doi:10.5194/acp-11-3137-2011, 2011.

Jimenez, J. L., Canagaratna, M. R., Donahue, N. M., Prevot, a. S. H., Zhang, Q., Kroll, J. H., DeCarlo, P. F., Allan, J. D., Coe, H., Ng, N. L., Aiken, a. C., Docherty, K. S., Ulbrich, I. M., Grieshop, A. P., Robinson, a. L., Duplissy, J., Smith, J. D., Wilson, K. R., Lanz, V. a., Hueglin, C., Sun, Y. L., Tian, J., Laaksonen, A., Raatikainen, T., Rautiainen, J., Vaattovaara, P., Ehn, M., Kulmala, M., Tomlinson, J. M., Collins, D. R., Cubison, M. J., Dunlea, J., Huffman, J. A., Onasch, T. B., Alfarra, M. R., Williams, P. I., Bower, K., Kondo, Y., Schneider, J., Drewnick, F., Borrmann, S., Weimer, S., Demerjian, K., Salcedo, D., Cottrell, L., Griffin, R., Takami, a., Miyoshi, T., Hatakeyama, S., Shimono, A., Sun, J. Y., Zhang, Y. M., Dzepina, K., Kimmel, J. R., Sueper, D., Jayne, J. T., Herndon, S. C., Trimborn, a. M., Williams, L. R., Wood, E. C., Middlebrook, A. M., Kolb, C. E., Baltensperger, U., Worsnop, D. R., Dunlea, E. J., Huffman, J. A., Onasch, T. B., Alfarra, M. R., Williams, P. I., Bower, K., Kondo, Y., Schneider, J., Drewnick, F., Borrmann, S., Weimer, S., Demerjian, K., Salcedo, D., Cottrell, L., Griffin, R., Takami, a., Miyoshi, T., Hatakeyama, S., Shimono, A., Sun, J. Y., Zhang, Y. M., Dzepina, K., Kimmel, J. R., Sueper, D., Jayne, J. T., Herndon, S. C., Trimborn, a. M., Williams, L. R., Wood, E. C., Middlebrook, A. M., Kolb, C. E., Baltensperger, U., Worsnop, D. R., Dunlea, J., Huffman, J. A., et al.: Evolution of Organic Aerosols in the Atmosphere, Science (80-.)., 326(5959), 1525–1529, doi:10.1126/science.1180353, 2009.

Kahn, R. A., Gaitley, B. J., Martonchik, J. V., Diner, D. J., Crean, K. A. and Holben, B.: Multiangle Imaging Spectroradiometer (MISR) global aerosol optical depth validation based on 2 years of coincident Aerosol Robotic Network (AERONET) observations, J. Geophys. Res. D Atmos., 110(10), 1–16, doi:10.1029/2004JD004706, 2005.

Koepke, P., Hess, M., Schult, I. and Shettle, E. P.: Global Aerosol Data Set., 1997.

Kreidenweis, S. M., Petters, M. D. and DeMott, P. J.: Single-parameter estimates of aerosol water content, Environ. Res. Lett., 3(3), 035002, doi:10.1088/1748-9326/3/3/035002, 2008.

Lowenthal, D. and Kumar, N.: Light scattering from sea-salt aerosols at interagency monitoring of protected visual environments (IMPROVE) sites, J. Air Waste Manag., 56(5), 636–642, doi:10.1080/10473289.2006.10464478, 2006.

Malm, C., Sisler, J. F. and Cahill, A.: Spatial and seasonal trends in particle concentration and optical extinction in the United States, , 99, 1347–1370, 1994.

Malm, W. C.: Spatial and monthly trends in speciated fine particle concentration in the United States, J. Geophys. Res., 109(D3), D03306, doi:10.1029/2003JD003739, 2004.

Malm, W. C. and Hand, J. L.: An examination of the physical and optical properties of aerosols collected in the IMPROVE program, Atmos. Environ., 41(16), 3407–3427, doi:10.1016/j.atmosenv.2006.12.012, 2007.

Malm, W. C. and Kreidenweis, S. M.: The effects of models of aerosol hygroscopicity on the apportionment of extinction, Atmos. Environ., 31(13), 1965–1976, doi:10.1016/S1352-2310(96)00355-X, 1997.

Mann, G. W., Carslaw, K. S., Spracklen, D. V., Ridley, D. A., Manktelow, P. T., Chipperfield, M. P., Pickering, S. J. and Johnson, C. E.: Description and evaluation of GLOMAP-mode: A modal global aerosol microphysics model for the UKCA composition-climate model, Geosci. Model Dev., 3(2), 519–551, doi:10.5194/gmd-3-519-2010, 2010.

Martin, R. V.: Global and regional decreases in tropospheric oxidants from photochemical effects of aerosols, J. Geophys. Res., 108(D3), 4097, doi:10.1029/2002JD002622, 2003.

Martin, S. T., Schlenker, J. C., Malinowski, A. and Hung, H.: Crystallization of atmospheric sulfate-nitrate-ammonium particles, , 30(21), 1–4, doi:10.1029/2003GL017930, 2003.

Martin, S. T., Rosenoern, T., Chen, Q. and Collins, D. R.: Phase changes of ambient particles in the Southern Great Plains of Oklahoma, Geophys. Res. Lett., 35(22), 1–5, doi:10.1029/2008GL035650, 2008.

Mishchenko, M. I., Dlugach, J. M., Yanovitskij, E. G. and Zakharova, N. T.: Bidirectional reflectance of flat, optically thick particulate layers: An efficient radiative transfer solution and applications to snow and soil surfaces, J. Quant. Spectrosc. Radiat. Transf., 63(2–6), 409–432, doi:10.1016/S0022-4073(99)00028-X, 1999.

Molenar, J. V: Analysis of the Real World Performance of the Optec NGN-2 Ambient Nephelometer, Vis. Air Qual. Aerosols Glob. Radiat. Balanc., 243–265, 1997.

Ng, N. L., Canagaratna, M. R., Zhang, Q., Jimenez, J. L., Tian, J., Ulbrich, I. M., Kroll, J. H., Docherty, K. S., Chhabra, P. S., Bahreini, R., Murphy, S. M., Seinfeld, J. H., Hildebrandt, L., Donahue, N. M., Decarlo, P. F., Lanz, V. A., Prévôt, A. S. H., Dinar, E., Rudich, Y. and Worsnop, D. R.: Organic aerosol components observed in Northern Hemispheric datasets from Aerosol Mass Spectrometry, Atmos. Chem. Phys., 10(10), 4625–4641, doi:10.5194/acp-10-4625-2010, 2010.

Pandolfi, M., Alados-arboledas, L., Andrade, M., Backman, J., Baltensperger, U., Bonasoni, P., Bukowiecki, N., Coen, C., Conil, S., Coz, E., Crenn, V., Dudoitis, V., Eleftheriadis, K., Favez, O., Fetfatzis, P., Fiebig, M., Ginot, P., Gysel, M., Henzing, B., Hoffer, A., Holubova, A., Kalapov, I., Kalivitis, N., Kouvarakis, G., Kristensson, A., Kulmala, M., Lihavainen, H., Lunder, C., Luoma, K., Lyamani, H., Mihalopoulos, N., Moerman, M., Dowd, C. O., Petit, J., Pichon, J. M., Prokopciuk, N., Putaud, J., Sciare, J., Sellegri, K., Stamenov, D. B., Swietlicki, E., Titos, G., Tuch, T., Tunved, P., Ulevicius, V., Vaishya, A., Virkkula, A., Vratolis, S., Weingartner, E., Wiedensohler, A. and Laj, P.: Discussion started : 13 October 2017 Manuscript under review for journal Atmos . Chem . Phys . Discussion started : 13 October 2017 c Author (s) 2017 . CC BY 4 . 0 License ., , (October), 2017.

Park, R. J.: Sources of carbonaceous aerosols over the United States and implications for natural visibility, J. Geophys. Res., 108(D12), 4355, doi:10.1029/2002JD003190, 2003.

Park, R. J., Jacob, D. J., Field, B. D., Yantosca, R. M. and Chin, M.: Natural and transboundary pollution influences on sulfate-nitrate-ammonium aerosols in the United States: Implications for policy, J. Geophys. Res. D Atmos., 109(15), doi:10.1029/2003JD00473, 2004.

Petters, M. D. and Kreidenweis, S. M.: A single parameter representation of hygroscopic growth and cloud\ncondensation nucleus activity, Atmos. Chem. Phys., 1961–1971, doi:10.5194/acp-7-1961-2007, 2007.

Petters, M. D. and Kreidenweis, S. M.: A single parameter representation of hygroscopic growth and cloud condensation nucleus activity-Part 3: Including surfactant partitioning, Atmos. Chem. Phys., 13(2), 1081–1091, doi:10.5194/acp-13-1081-2013, 2013.

Philip, S., Martin, R. V., Pierce, J. R., Jimenez, J. L., Zhang, Q., Canagaratna, M. R., Spracklen, D. V., Nowlan, C. R., Lamsal, L. N., Cooper, M. J. and Krotkov, N. A.: Spatially and seasonally resolved estimate of the ratio of organic mass to organic carbon, Atmos. Environ., 87, 34–40, doi:10.1016/j.atmosenv.2013.11.065, 2014.

Pye, H. O. T., Liao, H., Wu, S., Mickley, L. J., Jacob, D. J., Henze, D. J. and Seinfeld, J. H.: Effect of changes in climate and emissions on future sulfate-nitrate-ammonium aerosol levels in the United States, J. Geophys. Res. Atmos., 114(1), 1–18, doi:10.1029/2008JD010701, 2009.

Pye, H. O. T., Chan, A. W. H., Barkley, M. P. and Seinfeld, J. H.: Global modeling of organic aerosol: The importance of reactive nitrogen (NOx and NO3), Atmos. Chem. Phys., 10(22), 11261–11276, doi:10.5194/acp-10-11261-2010, 2010.

Rickards, A. M. J., Miles, R. E. H., Davies, J. F., Marshall, F. H. and Reid, J. P.: Measurements of the sensitivity of aerosol hygroscopicity and the κ parameter to the O/C ratio, J. Phys. Chem. A, 117(51), 14120–14131, doi:10.1021/jp407991n, 2013.

Ridley, D. A., Heald, C. L. and Ford, B.: North African dust export and deposition: A satellite and model perspective, J. Geophys. Res. Atmos., 117(2), 1–21, doi:10.1029/2011JD016794, 2012.

Singh, H. B., Brune, W. H., Crawford, J. H., Jacob, D. J. and Russell, P. B.: Overview of the summer 2004 Intercontinental Chemical Transport Experiment-North America (INTEX-A), J. Geophys. Res. Atmos., 111(24), doi:10.1029/2006JD007905, 2006.

Snider, G., Weagle, C. L., Martin, R. V., Van Donkelaar, A., Conrad, K., Cunningham, D., Gordon, C., Zwicker, M., Akoshile, C., Artaxo, P., Anh, N. X., Brook, J., Dong, J., Garland, R. M., Greenwald, R., Griffith, D., He, K., Holben, B. N., Kahn, R., Koren, I., Lagrosas, N., Lestari, P., Ma, Z., Vanderlei Martins, J., Quel, E. J., Rudich, Y., Salam, A., Tripathi, S. N., Yu, C., Zhang, Q., Zhang, Y., Brauer, M., Cohen, A., Gibson, M. D. and Liu, Y.: SPARTAN: A global network to evaluate and enhance satellite-based estimates of ground-level particulate matter for global health applications, Atmos. Meas. Tech., 8(1), 505–521, doi:10.5194/amt-8-505-2015, 2015.

Snider, G., Weagle, C. L., Murdymootoo, K. K., Ring, A., Ritchie, Y., Stone, E., Walsh, A., Akoshile, C., Anh, N. X., Balasubramanian, R., Brook, J., Qonitan, F. D., Dong, J., Griffith, D., He, K., Holben, B. N., Kahn, R., Lagrosas, N., Lestari, P., Ma, Z., Misra, A., Norford, L. K., Quel, E. J., Salam, A., Schichtel, B., Segev, L., Tripathi, S., Wang, C., Yu, C., Zhang, Q., Zhang, Y., Brauer, M., Cohen, A., Gibson, M. D., Liu, Y., Martins, J. V., Rudich, Y. and Martin, R. V.: Variation in global chemical composition of PM2.5: emerging results from SPARTAN, Atmos. Chem. Phys., 16(15), 9629–9653, doi:10.5194/acp-16-9629-2016, 2016.

Solomon, P. A., Crumpler, D., Flanagan, J. B., Jayanty, R. K. M., Rickman, E. E. and McDade, C. E.: U.S. National PM2.5 Chemical Speciation Monitoring Networks-CSN and IMPROVE: Description of Networks., J. Air Waste Manage. Assoc., 64(12), 1410–38, doi:10.1080/10962247.2014.956904, 2014.

Spracklen, D. V., Pringle, K. J., Carslaw, K. S., Chipperfield, M. P. and Mann, G. W.: A global off-line model of size-resolved aerosol microphysics: I. Model development and prediction of aerosol properties, Atmos. Chem. Phys., 5(8), 2227–2252, doi:10.5194/acp-5-2227-2005, 2005.

Stanier, C. O., Khlystov, A. Y. and Pandis, S. N.: Ambient aerosol size distributions and number concentrations measured during the Pittsburgh Air Quality Study (PAQS), Atmos. Environ., 38(20), 3275–3284, doi:10.1016/j.atmosenv.2004.03.020, 2004.

Tao, J., Zhang, L., Ho, K., Zhang, R., Lin, Z., Zhang, Z., Lin, M., Cao, J., Liu, S. and Wang, G.: Impact of PM 2 . 5 chemical compositions on aerosol light scattering in Guangzhou — the largest megacity in South China, Atmos. Res., 135–136, 48–58, doi:10.1016/j.atmosres.2013.08.015, 2014.

Titos, G., Foyo-Moreno, I., Lyamani, H., Querol, X., Alastuey, A. and Alados-Arboledas, L.: Optical properties and chemical composition of aerosol particles at an urban location: An estimation of the aerosol mass scattering and absorption efficiencies, J. Geophys. Res. Atmos., 117(4), 1–12, doi:10.1029/2011JD016671, 2012.

Trivitayanurak, W., Adams, P. J., Spracklen, D. V. and Carslaw, K. S.: Tropospheric aerosol microphysics simulation with assimilated meteorology: Model description and intermodel comparison, Atmos. Chem. Phys., 8(12), 3149–3168, doi:10.5194/acp-8-3149-2008, 2008.

Wang, J., Hoffmann, A. A., Park, R. J., Jacob, D. J. and Martin, S. T.: Global distribution of solid and aqueous sulfafte aerosols: Effect of the hysteresis of particle phase transitions, J. Geophys. Res. Atmos., 113(11), 1–11, doi:10.1029/2007JD009367, 2008.

Wang, Q., Jacob, D. J., Spackman, J. R., Perring, A. E., Schwarz, J. P., Moteki, N., Marais, E. A., Ge, C., Wang, J. and Barrett, S. R. H.: Global budget and radiative forcing of black carbon aerosol : Constraints from pole-to-pole (HIPPO) observations across the Pacific, , 119, 195–206, doi:10.1002/2013JD020824, 2014.

Wexler, A. S. and Clegg, S. L.: Atmospheric aerosol models for systems including the ions H + , NH 4 + , Na + , SO 4 2− , NO 3 − , Cl − , Br − , and H 2 O, J. Geophys. Res., 107(D14), 4207, doi:10.1029/2001JD000451, 2002.

White, W. H.: On the theoretical and empirical basis for apportioning extinction by aerosols: A critical review, Atmos. Environ., 20(9), 1659–1672, doi:10.1016/0004-6981(86)90113-7, 1986.

White, W. H., Macias, E. S., Nininger, R. C. and Schorran, D.: Size-resolved measurements of light scattering by ambient particles in the southwestern U.S.A., Atmos. Environ., 28(5), 909–921, doi:10.1016/1352-2310(94)90249-6, 1994.

Wise, M. E.: Hygroscopic growth of ammonium sulfate/dicarboxylic acids, J. Geophys. Res., 108(D20), 4638, doi:10.1029/2003JD003775, 2003.

Yu, F. and Luo, G.: Simulation of particle size distribution with a global aerosol model: Contribution of nucleation to aerosol and CCN number concentrations, Atmos. Chem. Phys., 9(20), 7691–7710, doi:10.5194/acp-9-7691-2009, 2009.

Zhang, L., Kok, J. F., Henze, D. K., Li, Q. and Zhao, C.: Improving simulations of fine dust surface concentrations over the western United States by optimizing the particle size distribution, Geophys. Res. Lett., 40(12), 3270–3275, doi:10.1002/grl.50591, 2013.

Page 39: [2] Deleted **Robyn Latimer** **10/24/18 4:29:00 PM**

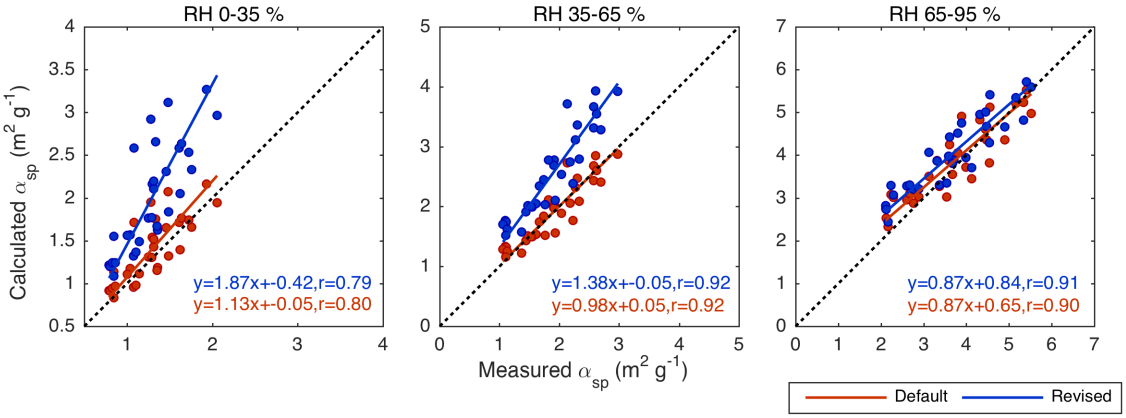

Page 40: [3] Deleted **Robyn Latimer** **10/24/18 4:29:00 PM**

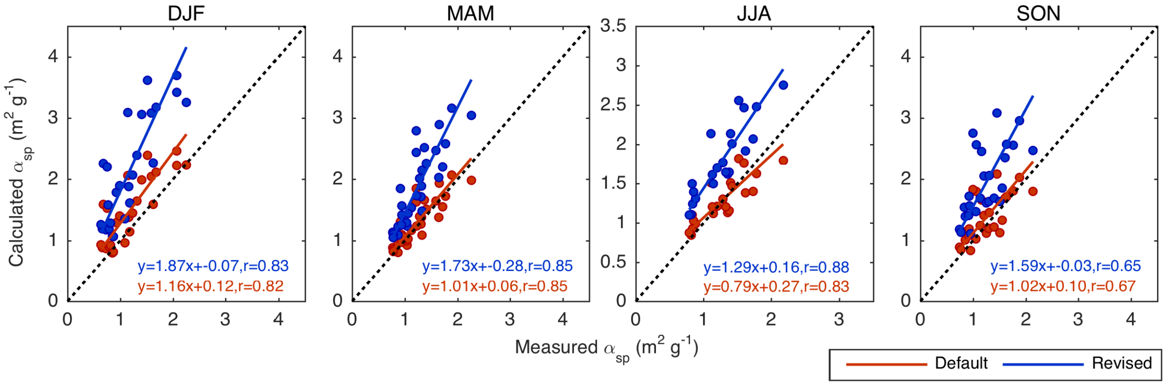

Page 43: [4] Deleted **Robyn Latimer** **10/28/18 7:06:00 PM**

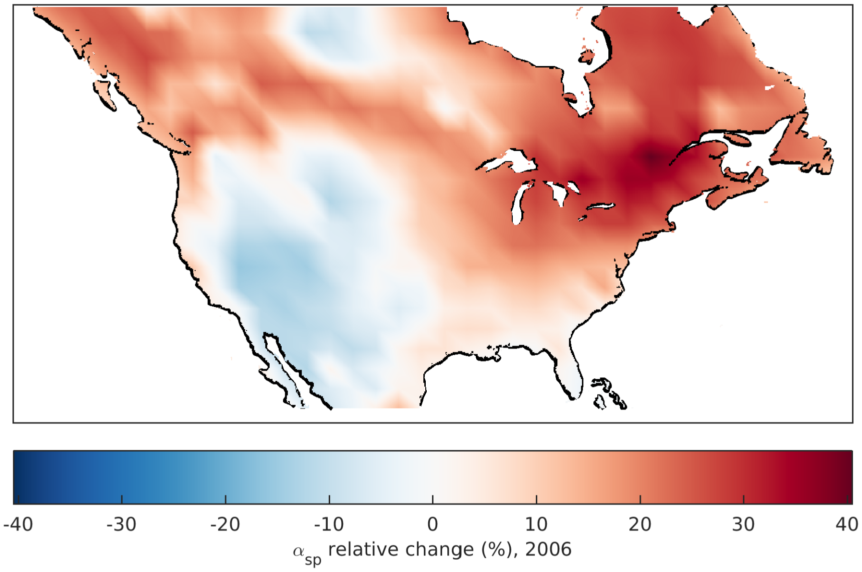

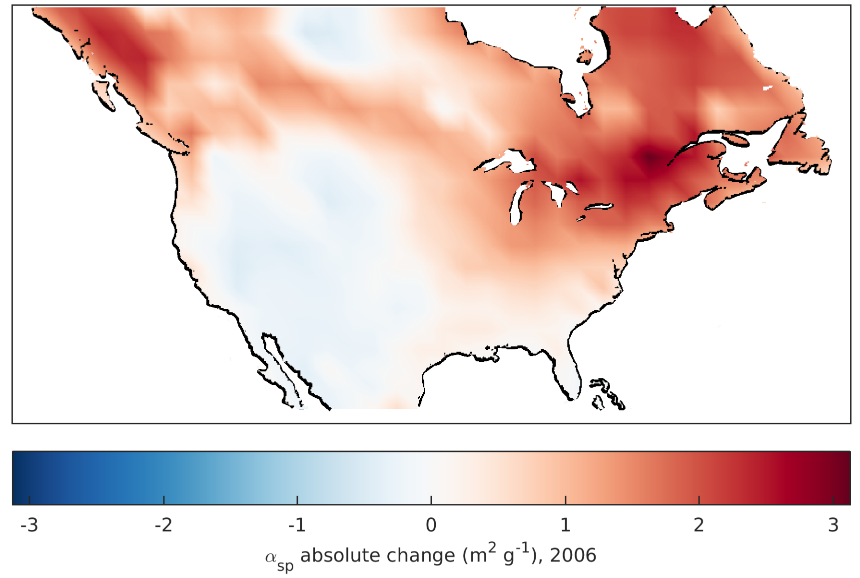

Page 46: [5] Deleted **Robyn Latimer** **10/28/18 7:07:00 PM**

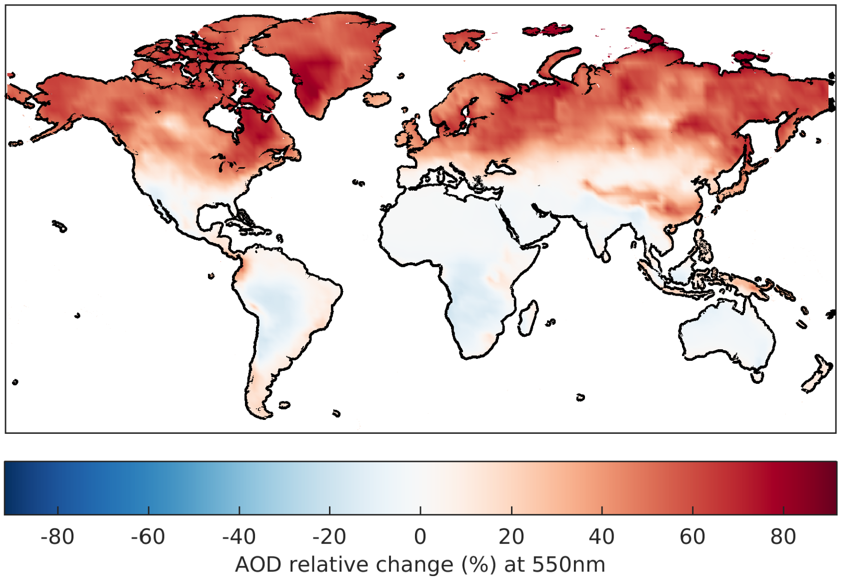

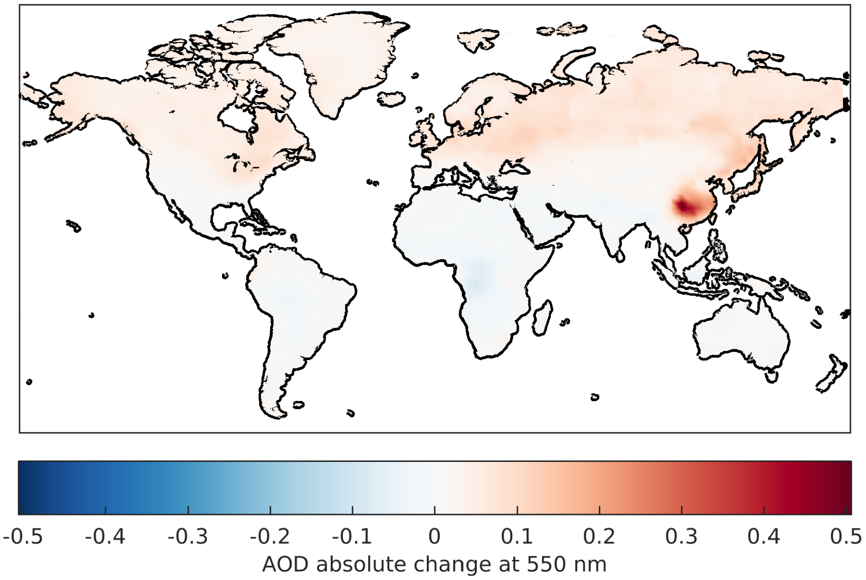

Page 50: [6] Deleted **Robyn Latimer** **10/28/18 7:07:00 PM**